

A two-step mechanism for epigenetic specification of centromere identity and function

Daniele Fachinetti¹, H. Diego Folco^{1,4}, Yael Nechemia-Arbely¹, Luis P. Valente², Kristen Nguyen¹, Alex J. Wong¹, Quan Zhu³, Andrew J. Holland^{1,4}, Arshad Desai¹, Lars E. T. Jansen² and Don W. Cleveland^{1,5}

1Ludwig Institute for Cancer Research and Department of Cellular and Molecular Medicine, University of California at San Diego, La Jolla, California 92093, USA. 2Instituto Gulbenkian de Ciência, Rua da Quinta Grande 6, P-2780-156, Oeiras, Portugal. 3Laboratory of Genetics, The Salk Institute for Biological Studies, La Jolla,

California 92037, USA. 4Present addresses: Laboratory of Biochemistry and Molecular Biology, National Cancer Institute, National Institutes of Health, Bethesda, Maryland 20892, USA (H.D.F.); Department of Molecular Biology and Genetics, Johns Hopkins University School of Medicine, Baltimore, Maryland 21205, USA (A.J.H.).

5Correspondence should be addressed to D.W.C. (e-mail: dcleveland@ucsd.edu) Received

The basic determinant of chromosome inheritance, the centromere, is specified in many eukaryotes by an epigenetic mark. Using gene targeting in human cells and fission yeast, chromatin containing the centromere-specific histone H3 variant CENP-A is demonstrated to be the epigenetic mark that acts through a two-step mechanism to identify, maintain and propagate centromere function indefinitely. Initially, centromere position is replicated and maintained by chromatin assembled with the centromere-targeting domain (CATD) of CENP-A substituted into H3. Subsequently, nucleation of kinetochore assembly onto CATD-containing chromatin is shown to require either the amino- or carboxy-terminal tail of CENP-A for recruitment of inner kinetochore proteins, including stabilizing CENP-B binding to human centromeres or direct recruitment of CENP-C, respectively.

The centromere is the fundamental unit for ensuring chromosome inheritance. Centromeres have a distinct type of chromatin in which histone H3 is replaced by a conserved homologue initially identified in humans and named CENP-A (refs 1,2). Although specific chromosomal regions containing α -satellite repeats³ are the sites of centromere formation and CENP-A association in humans, α -satellite DNA sequences are neither sufficient nor essential for centromere identity⁴. Rather, except for budding yeast, it is well accepted that in almost all other organisms, including fission yeast, centromeres depend on one or more as yet unidentified epigenetic marks⁵. Among the strongest evidence for an epigenetically defined centromere was the discovery in humans of migration of a functional centromere from an initial location to a new site on the same chromosome^{6–9}. These loci, referred to as neocentromeres, are stably loaded with CENP-A (ref. 8) and form at previous euchromatic DNA sites without α -satellite repeats^{6,10,11}. Epigenetic inheritance implies that the mark must be self-templating

and be stably maintained across the cell cycle. Centromere-bound CENP-A molecules are indeed quantitatively redistributed to both sister centromeres during centromeric DNA replication, yielding each daughter centromere with half the level of the initially loaded CENP-A (ref. 12). Furthermore, in human¹² and *Drosophila*^{13,14} cells, loading of new CENP-A into centromeric chromatin occurs once per cell cycle only during or on exit from mitosis.

Although the precise nature of centromeric chromatin is highly controversial^{15–24}, CENP-A is a central component in all models. Reduction or mutation in CENP-A (refs 25–28) has proved it to be essential for continuing centromere function²⁷. Indeed, forced loading of CENP-A by tethering it or components that bind it to specific DNA loci has produced partial ectopic centromere formation^{29–32} and in one case with full kinetochore function after deletion of the authentic centromere³³. These reports reinforce the sufficiency of CENP-A for recruitment of some centromere and kinetochore components, but offer no insight into how centromere identity and function are epigenetically specified and maintained. Approaches^{25–28} relying on RNA interference (RNAi)-mediated messenger RNA degradation to identify the epigenetic mark have suffered from incomplete silencing, especially for proteins such as CENP-A with long half-lives. To overcome these limitations, we now use gene targeting in human diploid cells and in fission yeast to demonstrate that CENP-A-containing chromatin is the epigenetic mark that can identify, maintain and propagate human or yeast centromere function indefinitely.

RESULTS

Conditional CENP-A gene deletion in diploid human cells

Using a single-stranded adeno-associated virus 2 (AAV2) vector to enhance homologous recombination^{34,35}, both human CENP-A alleles were targeted in non-transformed diploid human retinal epithelial (RPE1) cells immortalized with human telomerase. One allele was replaced with a CENP-A null allele in which a neomycin-resistance gene (flanked by FRT sites to facilitate its later removal) replaced exons 3 and 4 of the CENP-A gene (the exons encoding the essential CENP-A centromere targeting domain (CATD) that is comprised of loop 1 and the $\alpha 2$ helix of CENP-A and which when substituted into histone H3 is sufficient to restrict H3 targeting to centromeres³⁶). The other allele was specifically targeted with an AAV2 floxed construct containing 34-base-pair (bp) loxP recombination sites flanking exons 3 and 4 (Fig. 1a). This yielded a final cell line (CENP-A⁻/F) with one null allele and one floxed CENP-A allele, the latter of which can be converted into a null allele by action of Cre recombinase (Fig. 1a and Supplementary Fig. S1a). A CENP-A^F/+ cell line was also produced as a control. CENP-A⁻/F cells grew at a rate indistinguishable from the control CENP-A⁺/+ or CENP-A^F/+ with only a slight reduction of the total pool of CENP-A protein and no reduction seen at centromeres (Supplementary Fig. S1b–d). Transient expression of Cre recombinase (using a replication-defective adenoviral vector, Ad-Cre, to produce excision of exons 3 and 4 of the floxed allele (Supplementary Fig. S1e)) suppressed cell growth in the CENP-A⁻/F cells (Fig. 1b). PCR analysis of the few surviving clones revealed that they had escaped inactivation of the second CENP-A allele (Supplementary Fig. S1f). To eliminate confounding effects from these escapers, a LoxP-RFP-STOP-LoxP-GFP cassette was inserted (by lentiviral integration)

into the CENP-A^{F/+} and CENP-A^{-/F} cells (Supplementary Fig. S1g). Addition of Cre recombinase converted cells from red to green fluorescence by simultaneous excision of the RFP gene and activation of the GFP gene (Supplementary Video S1). CENP-A-depleted cells were then collected by fluorescence-activated cell sorting (FACS) to recover green fluorescent cells. After depletion of both alleles of CENP-A, cells duplicated at a similar rate as control cells for the first 5 days (~6 divisions), then exhibited slowed cycling from extended mitosis and stopped dividing only 9–11 days (~8–9 divisions) after initial CENP-A gene inactivation (Supplementary Fig. S1h). CENP-A excision led to progressive loss of accumulated CENP-A and its levels decreased by approximately half each cell cycle (Fig. 1c,d), consistent with the expected redistribution of centromere-bound CENP-A to sister centromeres during DNA replication but without addition of new CENP-A (ref. 12). Only 1% of the initial CENP-A level was detectable within 7 days (Fig. 1d; as expected for the 1/27 dilution = 0.8%). No centromere-bound CENP-A could be detected 9 days following excision (Fig. 1d). Lowered levels of CENP-A corresponded with increased rates of chromosome segregation defects and increased mitotic duration, accompanied by a significant increase in micronuclei formation from failure in initial kinetochore attachment to spindle microtubules or initially aligned chromosomes lagging in anaphase (Fig. 1e,f and Supplementary Video S2).

Disrupted kinetochore nucleation requires almost complete loss of CENP-A

CENP-A loading has been proposed to be at the foundation of recruitment (direct and indirect) of all of the components of the core centromere^{26,37–39}. Three patterns of centromere/kinetochore protein loss after inactivation of the conditional CENP-A allele in the CENP-A^{-/FRPE1} cells were identified in asynchronous cycling cells. The first group included: CENP-C and CENP-N, two primary components of the constitutive centromere-associated network (CCAN) that have been shown to directly interact with CENP-A chromatin^{37,38} and CENP-P, a more distal kinetochore protein³⁹. Loss of centromere-bound CENP-C, CENP-N and CENP-P was initially in proportion to loss of CENP-A (Fig. 2a,b,d and Supplementary Fig. S2a), consistent with direct binding to CENP-A chromatin or, in the case of CENP-P, through a CENP-N/CENP-C-dependent complex. Surprisingly, a substantial proportion (~30%) of CENP-C remained even after CENP-A depletion to <1% of its initial level (Fig. 2a,d). A second pattern included: CENP-T, a component of the CENP-T/W/S/X complex and whose histone fold domains bind to chromatin adjacent to centromeric CENP-A nucleosomes^{40,41}; CENP-I, which has been proposed to act in complex with CENP-H as another mediator of CENP-A deposition⁴²; and Ndc80, a direct microtubule-binding component of the outer kinetochore⁴³. Surprisingly, all three of these centromere/kinetochore proteins were almost fully maintained at centromeres (Fig. 2c,e and Supplementary Fig. S2b,c) until CENP-A levels dropped below ~1% of the initial level. Only after further loss of CENP-A were these kinetochore components then rapidly lost (Fig. 2e). A final group was represented by the direct DNA-binding protein CENP-B that recognizes a 17 bp sequence (CENP-B box) within α -satellite DNA (ref. 44). As expected, CENP-B binding at centromeres was not initially affected by reduction in CENP-A levels. Quite unexpectedly, however, CENP-B binding dropped by half as centromeric CENP-A was completely depleted (Fig. 2f), thereby identifying a previously unrecognized partial dependency on CENP-A for CENP-B binding at centromeres. Overall,

assessment of loss of kinetochore proteins as centromere-bound CENP-A was depleted identified that kinetochore assembly is not an all-or-nothing event and that a remarkably small amount of CENP-A is sufficient to nucleate assembly of a kinetochore with partial centromere function.

The CENP-A CATD maintains centromere position and templates its replication

Next we investigated whether CENP-A in centromeric chromatin can indefinitely maintain centromere identity by templating loading of new CENP-A onto replicated DNA of natural human centromeres and if so, the mechanism underlying its ability to do this. A series of histone H3 or CENP-A rescue variants were created with EYFP (enhanced yellow fluorescent protein) tags and stably expressed (by retroviral integration) in CENP-A-*-*/F cells (Fig. 3a,b and Supplementary Fig. S3a,b). The remaining CENP-A allele was then inactivated by addition of Ad-Cre. As expected, full-length CENP-A accumulated to the endogenous CENP-A level (Fig. 3c) and was able to support cell viability (Fig. 3d(i-ii),e). H3CATD rescued complete deletion of CENP-A with an efficiency 2/3 of CENP-A itself, whereas H3 alone conferred no survival (Fig. 3d(iii-iv),e). H3CATD continued to be loaded at centromeres at a constant level even 5–6 generations after reduction of CENP-A to below 1% of its normal level (see Discussion; Fig. 4a–c).

To determine whether CATD-dependent centromere identity was maintained through replication of centromeric chromatin at mitotic exit¹² and in an HJURP-dependent manner^{45,46} in the absence of endogenous CENP-A, a SNAP-tagged H3CATD construct was stably expressed in CENP-A-*-*/F cells. In cells treated with a control GAPDH short interfering RNA (siRNA), assembly of new SNAP-H3CATD molecules at centromeres was observed only at mitotic exit. This loading was completely dependent on HJURP, as its reduction abolished new SNAP-H3CATD assembly (Fig. 4d–f). Furthermore, in agreement with recent findings⁴⁷, the continued HJURP-dependent loading of H3CATD missing Ser 68 demonstrated that it is not necessary for CENP-A recognition and loading by HJURP, in contrast with a previous hypothesis⁴⁸. Whereas cell-cycle-dependent loading of new H3CATD at centromeres continued after CENP-A depletion, other centromeric proteins including CENP-I, CENP-N, CENP-C and CENP-T were inefficiently assembled at the CENP-A-depleted H3CATD-containing centromeres, although all but CENP-C were maintained longer when compared with cells with no rescue construct (Fig. 4c and Supplementary Fig. S3d). Failure to maintain or recruit kinetochore proteins caused a marked increase in chromosome segregation defects (Fig. 4g) that prevented long-term survival (>100 generations; Fig. 5a,b). Thus, substituting the CATD into histone H3 enables it to mediate epigenetic inheritance of centromere position through a mechanism requiring its cell-cycle-dependent recruitment by the chaperone/loader HJURP, but H3CATD-containing centromeric chromatin is not sufficient to nucleate assembly of a functional kinetochore.

N- or C-terminal tail of centromere-bound CENP-A enables long-term centromere rescue

We then investigated how CENP-A confers long-term centromere function. The α N helix of CENP-A has been shown to be important for contacting DNA as it exits a CENP-A-containing nucleosome^{19,49} and the six-amino-acid C-terminal tail of CENP-A can directly recruit CENP-C and drive aspects of kinetochore assembly in *in vitro* extracts²⁹. We therefore created stable cell lines expressing H3CATD with the addition of the CENP-A α N helix (α NH3CATD), C-terminal tail (H3CATD+C) or all or part of its N-terminal tail (NH2H3CATD or NH2(1–29)H3CATD; Fig. 3a and Supplementary Fig. S3a). Addition to H3CATD of either CENP-A tail rescued not only growth in the short-term assay—similar to the full-length CENP-A (Fig. 3d(v–vi),e and Supplementary Fig. S3c)—but also supported growth indefinitely (Fig. 5b), with only a mild slow growth phenotype relative to cells still containing the endogenous CENP-A (Supplementary Fig. S4a). Centromere function continued in the complete absence of CENP-A, as deletion of both endogenous CENP-A genes was confirmed by immunoblotting, PCR and immunofluorescence microscopy (Fig. 5c and Supplementary Fig. S4b,c). As expected, loading of the rescue constructs occurred only after mitotic exit and was dependent on HJURP (Supplementary Fig. S4d–f). Redundancy of the N- and C-terminal tails of CENP-A in supporting long-term viability was further confirmed by full rescue with CENP-A constructs deleted in either domain (H3–NH2CENP-A and CENP-AC–H3; Fig. 5b).

The CENP-A C-terminal tail directs CENP-C binding, but is not essential for kinetochore assembly

Our findings suggested that full kinetochore assembly was nucleated by recruitment by either tail domain of one or more components. Indeed, consistent with direct CENP-C recruitment by the CENP-A C-terminal tail²⁹, centromere-associated CENP-C was reduced in cells lacking the CENP-A C terminus (CENP-AC–H3 and NH2H3CATD; Fig. 5d,e). Nevertheless, a fraction of CENP-C remained centromere bound in cells rescued long-term in the absence of the C-terminal tail, demonstrating the existence of CENP-A C-terminal-independent loading of CENP-C, possibly through an existing CENP-C that templates new CENP-C loading. This remaining CENP-C was essential for centromere function, as depletion of it with siRNA produced catastrophic chromosome mis-segregation (Supplementary Fig. S4g). Similar reduction was also observed for CENP-I, suggesting its stabilization by CENP-C (Fig. 5e and Supplementary Fig. S5a). In any event, centromeres rescued with CENP-A variants missing its C-terminal tail (CENP-AH3–C and NH2H3CATD) were sufficient for long-term kinetochore function, with normal assembly of associated centromere proteins thereby maintaining centromere function (Fig. 5d,e and Supplementary Fig. S5a).

The CENP-A N-terminal tail controls CENP-B levels at centromeres

CENP-C, CENP-T, CENP-N, Ndc80 and Dsn1 were fully maintained at centromeres in the absence of CENP-A following long-term rescue with each variant missing the N-terminal CENP-A tail (H3–NH2CENP-A and H3CATD+C; Fig. 5d,e). Surprisingly, however, the CENP-A N-terminal tail was required for proper loading of the direct DNA-binding protein CENP-B. Without that N-terminal tail, only 50% of the normal centromeric amount of CENP-B was loaded at centromeres (Fig. 6a and Supplementary Fig. S5b). This CENP-A-dependent CENP-B binding was essential for centromere function. Indeed, stable reduction of total CENP-B by

half in CENP-A-deleted cells rescued by NH2H3CATD markedly increased chromosome mis-segregation and nearly eliminated colony survival (Fig. 6b,c and Supplementary Fig. S5c). Similar reduction in CENP-B did not affect rescue with full-length CENP-A, presumably because kinetochore functionality was still maintained through recruitment of CENP-C mediated by the C-terminal tail (Fig. 6b,c). Indeed, further reduction of CENP-B did not affect kinetochore function and survival of the H3CATD+C cells (Fig. 6c). This finding implicates CENP-B stabilization as one important component of kinetochore assembly nucleated in a manner dependent on the CENP-A N-terminal tail.

Accurate chromosome segregation with centromere-targeted histone H3 carrying either CENP-A tail domain

The degree of complementation of normal chromosome segregation in cells deleted in CENP-A and rescued with CENP-A or H3CATD including either CENP-A tail domain was measured using fluorescence in situ hybridization (FISH) to visualize chromosomes 2 and 7. No increase in aneuploidy was observed in CENP-A- or H3CATD+C-rescued cells and only a minor increase was found in NH2H3CATD-rescued cells (Fig. 6d). Direct visualization of chromosome segregation using time-lapse microscopy confirmed almost normal segregation in all rescued lines (Supplementary Fig. S5d,e). Overall, long-term, faithful centromere replication and kinetochore function was mediated by CATD-containing centromeric chromatin with either tail of CENP-A.

The principles of epigenetic centromere inheritance and function are conserved in fission yeast

We next tested the generality of our findings by examining whether the CATD and tail domains of CENP-A similarly specify centromere identity and kinetochore assembly in the fission yeast *Schizosaccharomyces pombe*, an organism whose epigenetically defined centromeres contain repeat motifs that are reminiscent of the repetitive arrays found at most higher eukaryotic centromeres⁵⁰. Various histone H3-CENP-ACnp1 rescue genes were constructed to test the contribution of the fission yeast CATD (which lies within the CENP-ACnp1 histone fold domain (HFD)), the short CENP-ACnp1 N-terminal tail (19 amino acids) and the remaining regions of the CENP-ACnp1 HFD that were not included in the CATD (for simplicity we refer to these as N-HFD and C-HFD; Fig. 7a). GFP- tagged chimaeric CENP-ACnp1 variants were expressed in a yeast strain bearing a tetO array inserted at centromere 2, as well as expressing a tetR-Tomato fusion protein that allows visualization of centromere 2 (Fig. 7c and Supplementary Table S1 and Fig. S6). H3CATD co-localized with the centromere, whereas a Cnp1 whose CATD was exchanged with the corresponding domain of histone H3 (Cnp1CATDswap) was found scattered throughout the nucleus (Fig. 7b,c). Chromatin immunoprecipitation confirmed enrichment of H3CATD, but not Cnp1CATDswap, specifically at centromeres relative to non-centromeric regions (Fig. 7b,d).

The ability of the various Cnp1 rescue constructs to complement

the complete absence of CENP-A was tested by employing a plasmid- shuffling assay (Fig. 7e). H3CATD was unable to confer cell viability, but addition of the Cnp1 N-terminal tail to H3CATD did sustain long-term viability (Fig. 7f). Similar results were observed when the rescue constructs were then introduced in cells harbouring a CENP-ACnp1 temperature-sensitive mutant allele (*cnp1-76*; ref. 51) as the unique source of CENP-A (Fig. 7g). There was no noticeable difference in growth rates among control cells expressing full-length Cnp1 or H3CATD with the Cnp1 N-terminal tail. Only a slight sensitivity was seen for cells rescued with the latter construct and exposed to drugs that drive spindle disassembly, indicating that centromere function is largely restored (Fig. 7h). In contrast with human, CENP-ACnp1 has only one amino-acid C-terminal extension beyond the end of the HFD (ref. 52). The corresponding rescue construct (H3CATD+C-HFD) did not maintain growth in the complete absence of CENP-ACnp1, although it did restore growth of the *cnp1-76* mutant at the restrictive temperature (Fig. 7f,g), probably facilitating the recruitment of the thermo-sensitive *cnp1-76* mutant to centromeres that in turn may recruit kinetochore components through its N-terminal tail. Thus, in fission yeast the CATD requires the addition of the Cnp1 N-terminal tail to provide long-term viability, as in human cells.

DISCUSSION

A long-standing question in chromosome inheritance is the epigenetic mark of centromere identity. By artificially targeting components to chromatin^{29–31,33}, several groups have demonstrated that large artificial arrays of CENP-A-containing chromatin are sufficient to generate partially functional centromeres, but only after completely abrogating any epigenetic component. One earlier effort had reduced CENP-A levels using siRNA (ref. 27). Such approaches fail to test the epigenetic question as they are plagued by partial suppression that precludes testing epigenetic sufficiency. Indeed, we now demonstrate that as little as 1% of the original CENP-A level is sufficient for retention of at least partial centromere function and assembly of kinetochore proteins. Our use of conditional gene inactivation in human cells and in fission yeast has overcome the previous technical limitations and

has now established that the CATD of CENP-A when substituted into histone H3 can template its cell-cycle-dependent, HJURP/Scm3- dependent centromeric loading at a constant level in the complete absence of CENP-A. Consideration of the number of molecules of CENP-A at the normal centromere offers strong support for this conclusion. The number of CENP-A molecules at the 40–500 kilobase chicken centromeres has been reported to be between 25 and 40 (ref. 53). Increasing that by tenfold to account for the increased centromere size in humans yields a maximal estimate of ~250–400 CENP-A molecules per centromere, with a corresponding prediction of <1 molecule remaining per centromere within 9 divisions after CENP-A gene inactivation (400 molecules per centromere \times $1/2^9$ = 0.8 molecules per centromere). Therefore, our evidence demonstrates that H3CATD continues to be loaded at its initial level at each centromere for 4–5 generations after the CENP-A level has fallen below ~1 molecule per centromere. It is important to note that initial H3CATD assembly occurs in the presence of endogenous CENP-A; therefore, our evidence offers no insight into de novo centromere formation. Despite its necessity and sufficiency for maintaining centromere

identity in the absence of CENP-A, we have shown that H3CATD is not sufficient for long-term centromere function and cell viability because it does not nucleate kinetochore assembly. Rather, we have identified two redundant pathways that function to initiate kinetochore assembly onto an epigenetically defined chromatin core containing the CATD. Our evidence establishes that CENP-A-containing chromatin is the epigenetic mark that can identify, maintain and propagate human centromere function indefinitely through a conserved two-step mechanism in which it templates its own CATD-dependent replication and nucleates subsequent kinetochore assembly (Fig. 8). Furthermore, we demonstrate that the principles of epigenetic centromere inheritance and function are conserved from human to fission yeast. The most plausible model is that the CATD establishes the epigenetic

mark by physically modifying centromeric chromatin⁵⁴ mediated by its interaction with histone H4 (ref. 21) and by the exposure of the positively charged Loop1 of the CATD (refs 21,22). Conformationally constrained CENP-A-containing chromatin and the exposed Loop1 can then attract centromeric components such as CENP-N or the

nucleosome-like CENP-T/W/S/X complex. Indeed, recognition of these chromatin features offers an explanation for the slow loss of CENP-Nor CENP-T from H3CATD-defined centromeres. Further, earlier evidence had shown that the C-terminal CENP-A

tail can recruit CENP-C in vitro and that this is sufficient to initiate assembly of kinetochore components that are capable of microtubule capture²⁹. Adding to that earlier work, our evidence has established that the human CENP-A C-terminal tail not only recruits CENP-C, but also is sufficient to nucleate functional kinetochore assembly required for high-fidelity chromosome segregation indefinitely when linked to a histone H3 variant with the CATD. Nevertheless, our evidence has also demonstrated that the CENP-A rescue construct lacking the CENP-A C-terminal tail still supports kinetochore assembly. Indeed, a fraction of CENP-C remains bound to centromeres even in the absence of the CENP-A C terminus, possibly through its proposed DNA-binding domain or interaction with histone H3 or CENP-B (refs 55–57). This underscores that the C-terminus of CENP-A is not essential for centromere function as previously suggested²⁹, although in its absence kinetochore function is slightly impaired, as observed by an increase in chromosome segregation errors and modestly increased aneuploidy. Regarding a previously unrealized influence of CENP-B on kinetochore assembly, binding of CENP-B had previously been reported to affect the formation of heterochromatin⁵⁸. Added to this, use of chromatin fibres and super-resolution microscopy had revealed CENP-A nucleosomes to be interspersed with chromatin containing H3K4me2 (ref. 59) or H3K9me3 (ref. 53) histone H3 modifications. In addition, evidence for CENP-B binding to the CENP-B box was demonstrated to include an effect on positioning of CENP-A nucleosomes on alphoid DNA (refs 60,61). Our evidence has uncovered that at least a fraction of the centromeric CENP-B that is dependent on the first 29 amino acids of the CENP-A N terminus is required for accurate chromosome segregation (in the absence of the parallel kinetochore formation pathway mediated by the CENP-A C-terminal tail). This provides direct evidence in support of a role for the N-terminal tail of CENP-A in centromere function and for

CENP-B in kinetochore assembly. Finally, we note that an essential impact of CENP-B on reinforcing CENP-A chromatin offers an explanation for the previous finding that the density of CENP-B boxes influences the assembly and maintenance of CENP-A chromatin in human cells⁶². Our findings, coupled with evidence that direct targeting of CENP-C to a specific DNA site is sufficient to recruit CENP-A to that site in chicken cells³³ (but not in human cells³², at least when the endogenous centromere is still present), are consistent with epigenetic centromere identity that is stabilized by CENP-C and CENP-B.

METHODS

Methods and any associated references are available in the online version of the paper. Note: Supplementary Information is available in the online version of the paper

ACKNOWLEDGEMENTS The authors would like to thank P. Jallepalli (Sloan-Kettering, New York, USA) for helpful suggestions, J. F. Mata and M. C. C. Silva (Gulbenkian Institute, Oeiras, Portugal), T. Panchenko (University of Pennsylvania, Philadelphia, USA)

for technical help, D. Foltz (University of Virginia, Charlottesville, USA), A. Straight (Stanford University, USA), P. Maddox (Université de Montréal, Canada), S-T. Liu (University of Toledo, USE), A. Miyawaki (RIKEN, Japan), R. Allshire (WTCCB, Edinburgh, UK), Y. Watanabe (University of Tokyo, Japan) and O. Limbo and P. Russell (TSRI, La Jolla, USA) for providing reagents. We also thank B. E. Black and C. Bartocci (TSRI, La Jolla) for helpful comments on the manuscript, E. Khaliullina for drawing the model in Fig. 8, the Neuroscience Microscopy Shared Facility (P30 NS047101, University of California, San Diego) and the FACS facility in the HESCCF (Sanford Consortium for Regenerative Medicine, La Jolla, CA). This work was supported by a grant (GM074150) from the National Institutes of Health to D.W.C., who receives salary support from the Ludwig Institute for Cancer Research. D.F. was supported by a European Molecular Biology Organization (EMBO) long-term fellowship.

AUTHOR CONTRIBUTIONS H.D.F. and A.D. designed and performed yeast experiments and contributed to manuscript writing. L.P.V. and L.E.T.J. performed FISH experiments. L.E.T.J. targeted the first CENP-A allele. D.F., Y.N.-A., K.N., A.J.W., Q.Z., A.J.H. performed the experiments. D.F. analysed the data. D.F. and D.W.C. conceived the experimental design and wrote the manuscript.

COMPETING FINANCIAL INTERESTS The authors declare no competing financial interests.

References

1. Palmer, D. K., O'Day, K., Wener, M. H., Andrews, B. S. & Margolis, R. L. A 17-kD centromere protein (CENP-A) copurifies with nucleosome core particles and with histones. *J. Cell Biol.* 104, 805815 (1987).

2. Earnshaw, W. C. & Rothel, N. Identification of a family of human centromere proteins using autoimmune sera from patients with scleroderma. *Chromosoma* 91, 313321 (1985).
3. Cleveland, D. W., Mao, Y. & Sullivan, K. F. Centromeres and kinetochores: from epigenetics to mitotic checkpoint signaling. *Cell* 112, 407421 (2003).
4. Karpen, G. H. & Allshire, R. C. The case for epigenetic effects on centromere identity and function. *Trends Genet.* 13, 489496 (1997).
5. Ekwall, K. Epigenetic control of centromere behavior. *Annu. Rev. Genet.* 41, 6381 (2007).
6. Du Sart, D. et al. A functional neo-centromere formed through activation of a latent human centromere and consisting of non-alpha-satellite DNA. *Nat. Genet.* 16, 144153 (1997).
7. Ventura, M. et al. Recurrent sites for new centromere seeding. *Genome Res.* 14, 16961703 (2004).
8. Amor, D. J. et al. Human centromere repositioning 'in progress'. *Proc. Natl Acad. Sci. USA* 101, 65426547 (2004).
9. Warburton, P. E. Chromosomal dynamics of human neocentromere formation. *Chromosome Res.* 12, 617626 (2004).
10. Depinet, T. W. et al. Characterization of neo-centromeres in marker chromosomes lacking detectable alpha-satellite DNA. *Hum. Mol. Genet.* 6, 11951204 (1997).
11. Warburton, P. E. et al. Immunolocalization of CENP-A suggests a distinct nucleosome structure at the inner kinetochore plate of active centromeres. *Curr. Biol.* 7, 901904 (1997).
12. Jansen, L. E., Black, B. E., Foltz, D. R. & Cleveland, D. W. Propagation of centromeric chromatin requires exit from mitosis. *J. Cell Biol.* 176, 795805 (2007).

13. Schuh, M., Lehner, C. F. & Heidmann, S. Incorporation of *Drosophila* CID/CENP-A and CENP-C into centromeres during early embryonic anaphase. *Curr. Biol.* 17, 237243 (2007).
14. Mellone, B. G. et al. Assembly of *Drosophila* centromeric chromatin proteins during mitosis. *PLoS Genet.* 7, e1002068 (2011).
15. Dimitriadis, E. K., Weber, C., Gill, R. K., Diekmann, S. & Dalal, Y. Tetrameric organization of vertebrate centromeric nucleosomes. *Proc. Natl Acad. Sci. USA* 107, 2031720322 (2010).
16. Furuyama, T. & Henikoff, S. Centromeric nucleosomes induce positive DNA supercoils. *Cell* 138, 104113 (2009).
17. Krassovsky, K., Henikoff, J. G. & Henikoff, S. Tripartite organization of centromeric chromatin in budding yeast. *Proc. Natl Acad. Sci. USA* 109, 243248 (2012).
18. Mizuguchi, G., Xiao, H., Wisniewski, J., Smith, M. M. & Wu, C. Nonhistone Scm3 and histones CenH3-H4 assemble the core of centromere-specific nucleosomes. *Cell* 129, 11531164 (2007).
19. Conde e Silva, N. et al. CENP-A-containing nucleosomes: easier disassembly versus exclusive centromeric localization. *J. Mol. Biol.* 370, 555573 (2007).
20. Camahort, R. et al. Cse4 is part of an octameric nucleosome in budding yeast. *Mol. Cell* 35, 794805 (2009).
21. Sekulic, N., Bassett, E. A., Rogers, D. J. & Black, B. E. The structure of (CENP-A-H4)₂ reveals physical features that mark centromeres. *Nature* 467, 347351 (2010).
22. Tachiwana, H. et al. Crystal structure of the human centromeric nucleosome containing CENP-A. *Nature* 476, 232235 (2011).
23. Zhang, W., Colmenares, S. U. & Karpen, G. H. Assembly of *Drosophila* centromeric nucleosomes requires CID dimerization. *Mol. Cell* 45, 263269 (2012).

24. Black, B. E. & Cleveland, D. W. Epigenetic centromere propagation and the nature of CENP-a nucleosomes. *Cell* 144, 471479 (2011).
25. Regnier, V. et al. CENP-A is required for accurate chromosome segregation and sustained kinetochore association of BubR1. *Mol. Cell Biol.* 25, 39673981 (2005).
26. Liu, S. T., Rattner, J. B., Jablonski, S. A. & Yen, T. J. Mapping the assembly pathways that specify formation of the trilaminar kinetochore plates in human cells. *J. Cell Biol.* 175, 4153 (2006).
27. Black, B. E. et al. Centromere identity maintained by nucleosomes assembled with histone H3 containing the CENP-A targeting domain. *Mol. Cell* 25, 309322 (2007).
28. Fujita, Y. et al. Priming of centromere for CENP-A recruitment by human hMis18alpha, hMis18beta, and M18BP1. *Dev. Cell* 12, 1730 (2007).
29. Guse, A., Carroll, C. W., Moree, B., Fuller, C. J. & Straight, A. F. In vitro centromere and kinetochore assembly on dened chromatin templates. *Nature* 477, 354358 (2011).
30. Barnhart, M. C. et al. HJURP is a CENP-A chromatin assembly factor suficient to form a functional de novo kinetochore. *J. Cell Biol.* 194, 229243 (2011).
31. Mendiburo, M. J., Padeken, J., Fulop, S., Schepers, A. & Heun, P. Drosophila CENH3 is suficient for centromere formation. *Science* 334, 686690 (2011).
32. Gascoigne, K. E. et al. Induced ectopic kinetochore assembly bypasses the requirement for CENP-A nucleosomes. *Cell* 145, 410422 (2011).
33. Hori, T., Shang, W. H., Takeuchi, K. & Fukagawa, T. The CCAN recruits CENP-A to the centromere and forms the structural core for kinetochore assembly. *J. Cell Biol.* 200, 4560 (2013).
34. Russell, D. W. & Hirata, R. K. Human gene targeting by viral vectors. *Nat. Genet.* 18, 325330 (1998).

35. Berdugo, E., Terret, M. E. & Jallepalli, P. V. Functional dissection of mitotic regulators through gene targeting in human somatic cells. *Methods Mol. Biol.* 545, 2137 (2009).
36. Black, B. E. et al. Structural determinants for generating centromeric chromatin. *Nature* 430, 578582 (2004).
37. Carroll, C. W., Milks, K. J. & Straight, A. F. Dual recognition of CENP-A nucleosomes is required for centromere assembly. *J. Cell Biol.* 189, 11431155 (2010).
38. Carroll, C. W., Silva, M. C., Godek, K. M., Jansen, L. E. & Straight, A. F. Centromere assembly requires the direct recognition of CENP-A nucleosomes by CENP-N. *Nat. Cell Biol.* 11, 896902 (2009).
39. Foltz, D. R. et al. The human CENP-A centromeric nucleosome-associated complex. *Nat. Cell Biol.* 8, 458469 (2006).
40. Nishino, T. et al. CENP-T-W-S-X forms a unique centromeric chromatin structure with a histone-like fold. *Cell* 148, 487501 (2012).
41. Hori, T. et al. CCAN makes multiple contacts with centromeric DNA to provide distinct pathways to the outer kinetochore. *Cell* 135, 10391052 (2008).
42. Okada, M. et al. The CENP-H-I complex is required for the efficient incorporation of newly synthesized CENP-A into centromeres. *Nat. Cell Biol.* 8, 446457 (2006).
43. Cheeseman, I. M., Chappie, J. S., Wilson-Kubalek, E. M. & Desai, A. The conserved KMN network constitutes the core microtubule-binding site of the kinetochore. *Cell* 127, 983997 (2006).
44. Masumoto, H., Masukata, H., Muro, Y., Nozaki, N. & Okazaki, T. A human centromere antigen (CENP-B) interacts with a short specific sequence in alphoid DNA, a human centromeric satellite. *J. Cell Biol.* 109, 19631973 (1989).
45. Dunleavy, E. M. et al. HJURP is a cell-cycle-dependent maintenance and deposition factor of CENP-A at centromeres. *Cell* 137, 485497 (2009).

46. Foltz, D. R. et al. Centromere-specific assembly of CENP-A nucleosomes is mediated by HJURP. *Cell* 137, 472484 (2009).
47. Bassett, E. A. et al. HJURP uses distinct CENP-A surfaces to recognize and to stabilize CENP-A/histone H4 for centromere assembly. *Dev. Cell* 22, 749762 (2012).
48. Hu, H. et al. Structure of a CENP-A-histone H4 heterodimer in complex with chaperone HJURP. *Genes Dev.* 25, 901906 (2011).
49. Panchenko, T. et al. Replacement of histone H3 with CENP-A directs global nucleosome array condensation and loosening of nucleosome superhelical termini. *Proc. Natl Acad. Sci. USA* 108, 1658816593 (2011).
50. Allshire, R. C. & Karpen, G. H. Epigenetic regulation of centromeric chromatin: old dogs, new tricks? *Nat. Rev. Genet.* 9, 923937 (2008).
51. Castillo, A. G. et al. Plasticity of ssion yeast CENP-A chromatin driven by relative levels of histone H3 and H4. *PLoS Genet.* 3, 12641274 (2007).
52. Torras-Llort, M., Moreno-Moreno, O. & Azorin, F. Focus on the centre: the role of chromatin on the regulation of centromere identity and function. *EMBO J.* 28, 23372348 (2009).
53. Ribeiro, S. A. et al. A super-resolution map of the vertebrate kinetochore. *Proc. Natl Acad. Sci. USA* 107, 1048410489 (2010).
54. Black, B. E., Brock, M. A., Bedard, S., Woods, V. L. Jr & Cleveland, D. W. An epigenetic mark generated by the incorporation of CENP-A into centromeric nucleosomes. *Proc. Natl Acad. Sci. USA* 104, 50085013 (2007).
55. Trazzi, S. et al. The C-terminal domain of CENP-C displays multiple and critical functions for mammalian centromere formation. *PLoS ONE* 4, e5832 (2009).
56. Sugimoto, K., Yata, H., Muro, Y. & Himeno, M. Human centromere protein C (CENP-C) is a DNA-binding protein which possesses a novel DNA-binding motif. *J.*

Biochem. 116, 877881 (1994).

57. Suzuki, N. et al. CENP-B interacts with CENP-C domains containing Mif2 regions responsible for centromere localization. *J. Biol. Chem.* 279, 59345946 (2004).

58. Okada, T. et al. CENP-B controls centromere formation depending on the chromatin context. *Cell* 131, 12871300 (2007).

59. Sullivan, B. A. & Karpen, G. H. Centromeric chromatin exhibits a histone modification pattern that is distinct from both euchromatin and heterochromatin. *Nat. Struct. Mol. Biol.* 11, 10761083 (2004).

60. Hasson, D. et al. The octamer is the major form of CENP-A nucleosomes at human centromeres. *Nat. Struct. Mol. Biol.* 20, 687695 (2013).

61. Tanaka, Y. et al. Human centromere protein B induces translational positioning of nucleosomes on alpha-satellite sequences. *J. Biol. Chem.* 280, 4160941618 (2005).

62. Okamoto, Y., Nakano, M., Ohzeki, J., Larionov, V. & Masumoto, H. A minimal CENP-A core is required for nucleation and maintenance of a functional human centromere. *EMBO J.* 26, 12791291 (2007).

63. Sakuno, T., Tada, K. & Watanabe, Y. Kinetochores are organized by cohesion within the centromere. *Nature* 458, 852858 (2009).

METHODS

Cell culture. hTERT RPE-1 (ATCC) cells were maintained at 37 °C in a 5% CO₂ atmosphere with 21% oxygen. hTERT RPE-1 cells were maintained in DMEM:F12 medium containing 10% fetal bovine serum (Clontech), 0.348% sodium bicarbonate, 100 U/ml penicillin, 100 U/ml streptomycin and 2 mM l-glutamine. Monastrol was used at 100 nM for 10 h.

CENP-A gene targeting. To generate the CENP-A^{ΔF} cell line, two rounds of gene targeting were performed. To generate the first conditional allele the left

homology arm (encompassing a total of 1,373 bp of the genomic CENP-A locus from 43 bp upstream of CENP-A exon 2 to 134 bp downstream of exon 4) was PCR amplified from BAC clone RP11-106G13, carrying the entire genomic CENP-A locus (Invitrogen) and cloned into the BamHI/SpeI sites of the Bluescript derivative pNY (ref. 35). A loxP site was inserted 102 bp upstream of exon 3, such that exons 3 and 4 were flanked between this loxP and a loxP present in pNY. The 1,042 bp right homology arm was amplified from the same BAC clone and runs from 351 bp upstream of exon 5 to 691 bp downstream of the beginning of exon 5 and was subcloned as an XhoI/KpnI fragment into the corresponding sites of pNY. The whole cassette encompassing the left arm, loxP, FRT, Neo cassette, FRT, right arm was cloned into the NotI sites of pAAV-LacZ, replacing the lacZ gene. The CENP-A knockout targeting construct was derived from this floxed construct by transformation into Cre-expressing Escherichia coli, thereby resulting in site-specific removal of exons 3 and 4. A second floxed allele was created by gene synthesis (GenScript) to create 9 polymorphic variants and inserted into the pBluescript derivative pNY using the same approaches as described above. The entire insert was then excised through NotI digestion and ligated to a pAAV vector backbone. Procedures for preparation of infectious AAV particles, transduction of hTERT-RPE1 cells and isolation of properly targeted clones were performed as described previously³⁵.

Generation of stable cell lines, siRNA and SNAP-tag. The different transgenes used in this study were introduced by retroviral delivery as described previously⁶⁴. Stable integrates were selected in 5 μ g ml⁻¹ puromycin or 10 μ g ml⁻¹ blasticidin S and single clones isolated using fluorescence activated cell sorting (FACS Vantage; Becton Dickinson). An RFP_STOP_GFP was integrated by lentiviral infection. siRNAs were introduced using Lipofectamine

RNAiMax (Invitrogen). A pool of four siRNAs directed against CENP-C (50-GCGAAUAGAUUAUCAAGGA-30 , 50-GAACAGAAUCCAUCACAAA-30 , 50-CGAAGUUGAUAGAGGAUGA-30 , 50-UCAGGAGGAUUCGTGAUUA-30), CENPB (50-CCAACAAGCUGUCUCCUA-30 , 50-GGACAUCAAGCUGAGUCA-30 , 50-GGAGGGUGAUGUUGAUAGU-30 , 50-GGCGGGAGUUCGAGGUCUU-30) or HJURP (targeting nucleotides 1,135_1,153, 1,225_1,243, 1,815_1,833 and 2,017_2,033 of the HJURP open reading frame) and a single siRNA directed against GAPDH (50-UGGUUUACAUGAUCCAAUA-30) were purchased from Dharmacon. Short hairpin RNA (shRNA) against CENP-B and 2 negative controls (an empty and a non-effective 29-oligonucleotide scrambled sequence) were obtained from OriGene. SNAP labelling was conducted as described previously¹².

Clonogenic colony assay and Adeno-Cre treatment. Cells were plated in a 12-well plate at 4×10^4 . The next day, cells were washed three times in DMEM:F12 medium containing 2% fetal bovine serum. Ad-Cre virus was added at a multiplicity of infection of 250 in 400μ l of DMEM:F12 medium containing 2% fetal bovine serum. After 3.5 h, cells were washed three times with DMEM:F12 medium containing 10% fetal bovine serum. After 2 days, 500 cells were plated in triplicate on a 10 cm² dish. After a further 14 days, colonies were fixed for 10 min in methanol and stained for 10 min using a crystal violet staining solution (1% crystal violet and 20% ethanol). The percentage of clonogenic survival was determined by dividing the number of colonies formed in the Ad-Cre-treated condition versus the untreated cells. For live-cell microscopy, immunoblot analysis or immunofluorescence staining, cells were plated at 4×10^5 on a 10 cm² dish.

Immunoblotting. For immunoblot analysis protein samples were separated by SDS-PAGE, transferred onto nitrocellulose membranes (BioRad) and then probed with DM1A (α -tubulin, 1:5,000), CENP-A (Cell Signaling, 1:1,000), GFP (Roche,

1:500), HJURP (Covance, 1:1,000; ref. 46), CENP-B (Abcam and Upstate, 1:1,000) or GAPDH (Abcam, 1:10,000). Proteins for fission yeast were extracted with 0.7N NaOH solution and probed with GFP (Roche, 1:500) and α -actin (ACTB, Proteintech, 1:4,000).

Immunofluorescence and live-cell microscopy. Cells were fixed in 4% formaldehyde at room temperature or in methanol at 20 °C for 10 min. Incubations with primary antibodies were conducted in blocking buffer for 1 h at room temperature using the following antibodies: CENP-A (Abcam, 1:1,500), CENP-T (1:5,000), CENP-C (Covance, 1:1,000), CENP-B (Abcam, 1:1,000), ACA (Antibodies Inc, 1:500), Ndc80 (Abcam, 1:1,000), CENP-I (a gift from S-T. Liu, University of Toledo, USA), Dsn1 (1:1,000) and α -tubulin (1:2,000). Immunofluorescence images were collected using a Deltavision Core system (Applied Precision). For quantification of centromere signal intensity, un-deconvolved two-dimensional maximum intensity projections were saved as un-scaled 16-bit TIFF images and signal intensities determined using MetaMorph (Molecular Devices). A 15_15 pixel circle was drawn around a centromere (marked by ACA staining) and an identical circle drawn adjacent to the structure (background). The integrated signal intensity of each individual centromere was calculated by subtracting the fluorescence intensity of the background from the intensity of the adjacent centromere. About 20 centromeres were averaged to provide the average fluorescence intensity for each individual cell. Centromere signal intensity was also quantified using an automated system⁶⁵. Aliquots treated with Ad-Cre were compared with untreated conditions (Day 0). For CENP-N and CENP-P_SNAP, untreated controls were processed at the same time of the Ad-Cre treatment (day 1 to day 9). For high-resolution spinning-disc fluorescence microscopy, cells were imaged using a $\times 60$ 1.4NA PlanApochromat oil lens on a spinning-disc confocal mounted on a Nikon TE2000-E inverted

microscope equipped with a solid-state laser combiner (ALC)_491nm and 561nm lines_a Yokogawa CSU10 head and a CCD (charge-coupled device) Clara camera (Andor Technology). Acquisition parameters, shutters and focus were controlled by iQ 1.10.0 software (Andor Technology). Z sections of 5_ 2mM were acquired at 5 min time intervals for RFP and/or EYFP and maximum intensity projection created using MetaMorph. Movies were assembled and analysed using QuickTime (Apple).

Fluorescence in situ hybridization. Fluorescence in situ hybridization was performed as previously described²⁸ with the following alterations: centromerespecific probes for chromosomes 2 and 7 were labelled with tetramethyl-rhodamine-5-dUTP and Fluorescein-12-dUTP (Roche), respectively and coverslips were washed in 2_ SSC containing 60% formamide. More than 100 cells were analysed for each data point.

Yeast strain and plasmid construction. Standard procedures were used for bacterial and fission yeast growth, genetics and manipulations⁶⁶. CENP-Acnp1/H3 chimaeric constructs were obtained by a combination of DNA synthesis (GenScript), PCR and subsequent subcloning into standard LEU2-marked pREP81 plasmids. The codon usage of all constructs was optimized to the initial CENP-Acnp1 gene codon usage (Leto software). *S. pombe* strains used in this study are described in Supplementary Table S1. Cells were grown at 30 _C in all the experiments unless indicated otherwise. To create a cnp11 strain, a standard auxotrophic strain P013 was transformed with an ura4+-marked plasmid pREP82-cnp1+, thereby producing P162. P162 was subsequently transformed with a NAT cassette replacing the entire cnp1 ORF and thus obtaining a ura+ NATr strain, P164, which was checked by DNA blot and transformed with the aforementioned pREP81-based plasmids harbouring chimaeric constructs. Finally, transformants were employed in plasmid-shuffling

assays by plating serial dilution in PMG \square LEUCFOA (containing 50 μ g ml $^{-1}$ uracil) and PMG \square LEU \square URA as control plates. For the *cnp1-76* (ts) complementation assay, P482 strain was transformed with the mentioned pREP81-based plasmids. *leu+* transformants were isolated and analysed by serial dilution assays on PMG \square LEU at 25 $^{\circ}$ C and 36 $^{\circ}$ C. To isolate *cnp11*-harbouring pREP81-based plasmids as a unique source providing CENP-ACnp1, FOA-resistant colonies were picked directly from the plasmid-shuffling assay plate and subjected to two rounds of streaking onto PMG \square LEUCFOA. Loss of the *ura+* marker (that is, *cnp1+* plasmid) was confirmed. Subsequently, newly isolated strains were assessed by dilution serial assays on PMG containing thiabendazole (TBZ) at 15 μ g ml $^{-1}$ for 4 days at 30 $^{\circ}$ C.

S. pombe live-imaging. Cells were grown overnight until logarithmic phase in minimal medium PMG \square LEU at 30 $^{\circ}$ C and then mounted in PMG2% agarose. Cells were imaged on a spinning-disc microscope with a \times 100 1.4NA PlanApochromat oil lens on a spinning-disc confocal mounted on a Nikon TE2000-E inverted microscope equipped with a solid-state laser combiner (ALC) \square 491nm and 561nm lines \square a Yokogawa CSU10 head and a CCD Clara camera (Andor Technology). Fourteen 0.5- μ m z sections were acquired and further image processing, including maximum intensity projections, was performed using ImageJ (National Institutes of Health).

Chromatin immunoprecipitation. Cells were grown at 30 $^{\circ}$ C in PMG \square LEU. For each immunoprecipitation, 1 μ l of anti-GFP (A11122, Invitrogen) was used. Chromatin immunoprecipitation was performed as described previously⁶⁷ with the following modifications. After incubating the samples (that is, crude extracts and beads) with 250 μ l of TES for 6 h at 65 $^{\circ}$ C, 220 μ l of TE and 30 μ l of proteinase K (10 mg ml $^{-1}$) were added for subsequent overnight incubation at 37 $^{\circ}$ C. The following day, 3 volumes of PB buffer (Qiagen) were added and samples were

purified with Qiagen PCR purification kit as indicated by the manufacturer.

64. Shah, J. V. et al. Dynamics of centromere and kinetochore proteins;

implications for checkpoint signaling and silencing. *Curr. Biol.* 14,

942_952 (2004).

65. Bodor, D. L., Rodriguez, M. G., Moreno, N. & Jansen, L. E. Analysis of protein

turnover by quantitative SNAP-based pulse-chase imaging. *Curr. Protoc. Cell Biol.*

Chapter 8, Unit 8 (2012).

66. Moreno, S., Klar, A. & Nurse, P. Molecular genetic analysis of

yeast *Schizosaccharomyces pombe*. *Methods Enzymol.* 194,

795_823 (1991).

67. Folco, H. D., Pidoux, A. L., Urano, T. & Allshire, R. C. Heterochromatin and

RNAi are required to establish CENP-A chromatin at centromeres. *Science* 319,

94_97 (2008).

Figure 1 CENP-A conditional disruption in human cells. (a) Schematic

illustration of the final CENP-A cell lines after gene targeting. Positions

of the exons, the CATD domain, LoxP sites, FRT sites, the neomycin

cassette and the start/stop codons are indicated. Xs indicate polymorphic

mutations between the initial two CENP-A alleles. KO, knockout.

(b) Clonogenic cell survival assays (visualized with crystal violet) for

the indicated cell lines with (Ad-Cre) or without (NT, not treated)

treatment. (c) CENP-A protein level determined by immunoblotting

extracts from CENP-A^{+/+} and CENP-A^{+/F} cells at the indicated days after

Ad-Cre addition. (d) Top, representative fluorescence images of CENP-A

localization and intensity at the indicated days after Ad-Cre addition.

Bottom, quantification of CENP-A protein levels from fluorescence images.

Bars represent the mean of six independent experiments (>30 cells per experiment). Error bars represent the s.e.m. (standard error of the mean). ACA (anti-centromere antibody) staining was used to identify centromeres. (e) Time-lapse images of CENP-A^Δ=F RPE1 cells stably expressing histone H2B_mRFP 5 days after Ad-Cre addition. Time (in minutes) after nuclear envelope breakdown (NEBD) is shown at the top. Yellow arrows point to a lagging chromosome that ultimately forms a micronucleus. (f) Bars represent the mean of >50 cells per condition. Each individual point represents a single cell. Error bars represent the s.e.m. of three independent experiments. Time in mitosis was defined as the period from NEBD to chromosome decondensation. Uncropped images of blots are shown in Supplementary Fig. S7. Scale bar, 5 μm.

Figure 2 Disrupted centromere positioning and kinetochore nucleation requires almost complete loss of CENP-A. (a_c) Left, representative fluorescence images show the localization and intensity of CENP-A and CENP-C (a), CENP-N (b) and CENP-T (c) at day 0 and 7 or 9 after Ad-Cre addition to inactivate the remaining CENP-A allele in CENP-A^Δ=F cells. Right, bar graphs (the mean of four independent experiments; >30 cells per experiment) show CENP-A (red), CENP-C (green), CENP-N (orange) and CENP-T (blue) levels 0 to 9 days after Ad-Cre addition. Error bars represent the s.e.m. ACA staining was used to identify centromeres. CENP-N was tracked by covalent labelling with rhodamine-benzyl guanine after stable expression of a gene encoding SNAP-tagged CENP-N. (d_f) Kinetics of loss from centromeres as CENP-A levels diminish defines three groups with similar kinetics of loss: proteins lost in proportion to CENP-A (d), those lost more slowly and whose depletion

requires complete loss of CENP-A (e), and CENP-B (f), whose binding is reduced by half by complete loss of CENP-A. Statistics source data are in Supplementary Table S2. Scale bar, 5 μ m.

Figure 3 Short-term rescue of centromere maintenance and function following CENP-A gene depletion. (a) Schematic representation of the rescue constructs. Each CENP-A domain is in red; H3 in green. CENP-A domains and amino-acid positions are also indicated. Each construct is tagged with an N-terminal EYFP (enhanced yellow fluorescent protein). (b) Schematic outlining the construction of cell lines expressing each rescue construct and clonogenic assay. (c) Immunoblots of cell extracts with antibodies against GFP, CENP-A and α -tubulin to determine the level of expression of the indicated rescue constructs. (d) Clonogenic survival experiment for the indicated cell lines with or without addition of Ad-Cre. (e) Quantification of clonogenic assays for each rescue construct shown as the mean of the percentage of Ad-Cre-surviving colonies relative to the untreated condition. Each column represents the average of five independent experiments and error bars represent the s.e.m. Uncropped images of blots are shown in Supplementary Fig. S7.

Figure 4 H3CATD is sufficient for centromere identity and to template its chromatin replication. (a) Representative schematic of experimental design in b. (b) Representative fluorescence images of the localization and intensity of endogenous CENP-A and EYFP_H3CATD at days 0, 9 and 12 after Ad-Cre addition. ACA staining was used to identify

centromeres. (c) Bar graphs indicate protein intensity at centromeres of CENP-C, CENP-T, CENP-I, CENP-N and EYFP_H3CATD (in b) at the indicated days after Ad-Cre treatment. Columns represent the mean of ≥ 3 independent experiments (>30 cells per experiment) and error bars represent the s.e.m. (d) HJURP and GAPDH levels in cells with or without siRNA treatment for GAPDH or HJURP, determined by immunoblotting. α -tubulin was used as a loading control. (e) Representative schematic of experimental design in f. (f) Representative fluorescence images from the experiment in e to determine the localization and intensity of CENP-A and SNAP-H3CATD after siRNA of GAPDH or HJURP. α -tubulin staining was used to identify telophase-early G1 cells. (g) Columns are the mean of the percentage of micronuclei formation in CENP-A Δ C-F cells rescued with EYFP_H3CATD at the indicated days after Ad-Cre addition. Error bars represent the s.e.m. of three independent experiments (>100 cells per experiment). Statistics source data are in Supplementary Table S2. Uncropped images of blots are shown in Supplementary Fig. S7. Scale bars, 5 μ m.

Figure 5 N- or C-terminal tails of CENP-A nucleate kinetochore assembly.

(a) Schematic of the long-term viability assay used to isolate survival clones after endogenous CENP-A depletion. (b) Table of viability of various CENP-A_histone H3 chimaera for conferring short- (12_19 generations) and long-term (>100 generations) survival. (c) Immunoblot to quantify levels of each EYFP-tagged rescue variant or endogenous CENP-A, visualized with GFP or CENP-A antibodies. α -tubulin was used as a loading control. (d) Representative fluorescence images show the

localization and intensity of CENP-C or CENP-T in the indicated cell lines. ACA was used to mark centromeres. (e) Column graphs quantifying centromere intensities from experiments such as those in d to measure CENP-C, CENP-T, CENP-I, Ndc80 and Dsn1 protein intensity in the indicated cell lines. Columns represent the mean of three independent experiments (>30 cells per experiment). Error bars represent the s.e.m. Uncropped images of blots are shown in Supplementary Fig. S7. Scale bar, 5 μ m.

Figure 6 The CENP-A N-terminal tail controls CENP-B levels at centromeres.

(a) Column graphs represent the means of the percentage of CENP-B intensity in the indicated cell lines. Error bars represent the s.e.m. of three independent experiments (>30 cells per experiment. $P < 0.006$).

(b) Left, clonogenic survival assays after stable insertion to express a control shRNA (scramble) or against CENP-B. Right, immunoblot of cell extracts to measure total CENP-B levels. α -tubulin was used as a loading control. (c) Percentage of cells that undergo chromosome mis-segregation after GAPDH or CENP-B depletion by siRNA in the indicated cell line. Column graphs represent the means of three independent experiments and error bars represent the s.e.m. (d) Faithfulness of chromosome segregation after growth for 30 generations measured with FISH for centromere regions of chromosomes 2 and 7 (CEN2 and CEN7, respectively) in the presence (CENP-A^{ΔF}) or absence (CENP-A^{ΔT}) of endogenous CENP-A. Bars represent the mean of duplicate experiments in the indicated cell line (>100 cells per experiment). Bottom, diploid or aneuploid cells identified by localization of CEN2 (red) and CEN7 (green) after growth of the

CENP-A^Δ=ΔCNH2 H3CATD cells. Statistics source data are in Supplementary Table S2. Uncropped images of blots are shown in Supplementary Fig. S7a. Scale bar, 5 μm.

Figure 7 The *ssion* yeast CATD is necessary and sufficient for centromere identity, but requires addition of the CENP-ACnp1 N terminus to provide long-term centromere function. (a,b) Schematic of the CENP-ACnp1-histone H3 gene constructs (a) and the experimental approach used to test maintenance of centromere position and function in the *ssion* yeast *S. pombe* (b). CENP-ACnp1 domains are red; H3 in green. ChIP, chromatin immunoprecipitation. (c) Representative live-cell imaging of GFP-tagged constructs as outlined in b. The position of the centromere of chromosome 2 was marked by binding of a tetR-tomato fusion protein to a tetO array inserted at the central core of *cen2* (ref. 63). (d) Chromatin immunoprecipitation using GFP antibody of cells from b. Wild-type cells were transformed with GFP-tagged constructs as indicated. Enrichment at centromeric central cores (*cc1/3* and *cc2* products) was compared with input DNA relative to the control non-centromeric locus *fbp1*. The depiction of *ssion* yeast chromosomes is not drawn to scale. (e) Schematic of plasmid-shuffling assay for testing CENP-ACnp1 rescue constructs in *cnp11* cells. (f,g) Rescue experiment of *cnp11* cells using the plasmid-shuffling assay outlined in e or of *cnp1-76* cells. (h) Serial dilution of *cnp11* cells containing NH2H3CATD or CENP-ACnp1 as the unique source of CENP-ACnp1. Growth was assayed in *pombe* minimal medium with glutamate (PMG) with or without the addition of a spindle poison drug thiabendazole (TBZ; 15 μg ml⁻¹). Wild-type, *clr41* (heterochromatin defective mutant) and *cnp1-ts* controls are also shown. In f-h, a tenfold dilution series is shown

for each strain.

Figure 8 Model for centromeric identity, maintenance and function through a two-step mechanism. In the first step, centromere identity is achieved by the CATD-containing chromatin through its loading mediated by HJURP at mitotic exit. Subsequently, new and old CENP-A can nucleate kinetochore assembly on CATD-containing chromatin through the action of the CENP-A N-terminal tail that stabilizes CENP-B or by the direct recruitment of CENP-C by the C-terminal tail of CENP-A.

Figure S1 *CENP-A conditional disruption in human cells.* (a) CENP-A genotypes validated in the indicated cell lines using PCR to distinguish normal (+), disrupted (-), and floxed (F) alleles, as diagramed to right. (b) To monitor growth rate, CENP-A^{+/+}, CENP-A^{F/+} and CENP-A^{-/F} RPE1 cells were counted every 2 days. Values represent the mean of three independent experiments, and error bars represent the SEM. (c) Immunoblot to determine CENP-A levels in CENP-A^{+/+}, CENP-A^{F/+} and CENP-A^{-/F} RPE1 cells. (d) Representative fluorescence images of centromeric CENP-A levels. Bar graphs show CENP-A protein intensity in the indicated cell lines. Bars represent the mean of three independent experiments (> 30 cells per experiment). Error bars represent the SEM. ACA staining was used to identify centromeres in CENP-A^{F/+} and CENP-A^{-/F} RPE1 cells. (e) Efficiency of excision of exons 3 and 4 in the overall cell population determined by Q-PCR after Ad-Cre transduction of CENP-A^{-/F} RPE1 cells. Position of the primers is illustrated in the schematic at top. (f) PCR analysis on the DNA extracted from the survival colonies in the CENP-A^{-/F} RPE1

cells after Ad-CRE treatment. Images show representative crystal violet-stained colonies for the indicated cell lines with or without treatment with Ad-CRE.

(g) Schematic of introduction of the *LoxPRFP-STOPLoxP-GFP* gene by retroviral integration into CENP-A-/F cells, followed by FACS sorting to isolate only green fluorescing cells with both CENP-A alleles inactivated. (h) Graph shows the growth rate of CENP-AF/+ and CENP-A-/F with RFP-STOP-GFP construct of the experiment described in f. A parallel-untreated control is also shown. Cells were counted every 2 days. Values represent the mean of three independent experiments, and error bars represent the SEM. Scale bar = 5 mm.

Figure S2 Centromeric proteins dissociate from centromeres with different kinetics during CENP-A depletion. (a) Representative fluorescence images show the localization and intensity of CENP-P (purple bars). ACA staining was used to identify centromeres. Red bars show CENP-A intensity from Figure 1E. Bars represent the mean of three independent experiments (> 30 cells per experiment). Error bars represent the SEM. CENP-P was tracked by covalent labeling with rhodamine-benzyl guanine after stable expression of a gene encoding SNAP-tagged CENP-P (b) As in A, except that CENP-C and Ndc80 at day 0 and 7 are shown after Ad-Cre infection. Cells were arrested in monostanol for 12 hours. Yellow bars show Ndc80 intensity of the fluorescence images at the indicated days after Ad-Cre treatment. (c) As in a, but for CENP-A and CENP-I levels at day 0 and 9 after Ad-Cre infection. Interphase cells were quantified. Statistics source data are in supplementary table S2. Scale bar = 5 mm.

Figure S3 Clonogenic and immunofluorescence localization assays

determine that the CATD is sufficient for centromere identity and for templating its replication. (a) CENP-A amino acid sequence and the domains, including the amino terminal tail (red), the aN helix (green), the CATD (light blue), and the carboxyl terminal tail (orange). (b) Representative fluorescence images of the localization of EYFP-rescue constructs of experiment outlined in Figure 3. (c) Clonogenic survival assays (as in Figure 3d) for the CENP-A-/F cells with and without incubation in Ad-Cre and with the indicated rescue constructs. (d) Representative fluorescence images of the localization and intensity of CENP-T, CENP-A and EYFP-H3CATD at the indicated days after Ad-Cre treatment. Scale bar = 5 μ m.

Figure S4 H3CATD combined with either the amino or carboxyl tails of human

CENP-A confer long term centromere identity and kinetochore function.

(a) (Top) Clonogenic survival assays for RPE1 cells with the indicated CENP-A genotypes and rescue constructs. (Bottom) Corresponding growth rates determined by counting cell numbers every 2 days for CENP-A-/F cells and CENP-A-/- cells with CENP-A, NH₂H3CATD, or H3CATD-C rescue genes. Values represent the mean of three independent experiments, and error bars represent the SEM. (b) Confirmation of excision of endogenous CENP-A alleles in the indicated survival rescue construct cells. A schematic representation of the position of the primers is also shown. (c) (Top) Representative fluorescence images show the loss of endogenous CENP-A at centromeres only for cells lacking the amino-terminus of CENP-A epitopes recognized by our CENP-A antibody. ACA staining was used to identify centromeres. (Bottom) Quantitation of the fluorescence images in the

CENP-A^{-/-} + H3CATD-C and CENP-A^{-/-} + NH₂CENP-A cells. (d) Representative fluorescence images showing localization of the NH₂H3CATDSNAP in CENP-A^{-/-} cells during different phases of the cell cycle. ACA staining was used to identify centromeres and α-tubulin to identify telophase/early G1 cells. (e) Indirect immuno-fluorescence images of localization and intensity of EYFP-H3CATD-C at centromeres after GAPDH or HJURP siRNA, respectively. ACA staining was used to identify centromeres. (f) Quantitation of EYFP intensity at centromeres in images from (e) after GAPDH, HJURP siRNA, or no siRNA. Error bars represent the SEM of two independent experiments (> 30 cells per experiment). ACA staining was used to identify centromeres. (g) (Left) CENP-C protein intensity after GAPDH or CENP-C siRNA in the indicated cell lines, respectively. Bars represent the mean of two independent experiments (> 30 cells per experiment). (Right) Percentage of cells that undergo division after 72 hours of CENP-C depletion, determined by live cell microscopy. Error bars represent the SEM. Statistics source data are in supplementary table S2. Scale bar = 5 μm.

Figure S5 Accurate chromosome segregation with centromere-targeted histone H3 carrying either CENP-A tail domain. (a) Representative fluorescence images of localization and intensity of centromere-bound CENP-I or Ndc80 in CENP-A^{-/-} cell lines with the indicated rescue genes. ACA staining (red) is also shown. (b) Representative fluorescence images showing localization and intensity of centromere bound CENP-B in the indicated cell lines. (c) Representative fluorescence images showing localization and intensity of CENP-B in the indicated cell lines after 2

days of shRNA against CENP-B. (Right) Quantitation of CENP-B protein intensity of fluorescence images. (d) Time-lapse images of CENP-A-/-+ EYFPNH2H3CATD (green) RPE1 cells also stably expressing histone H2BmRFP (red). Numbers at the top right refer to the time in minutes after nuclear envelope breakdown (NEBD). Yellow arrows show the formation of micronuclei. (e) (Left) Quantitation of misaligned or lagging chromosomes or subsequent micronuclei formation or (right) mitotic timing, determined from images in (d). Time in mitosis was defined by the period from NEBD to chromosome decondensation. Bars represent the mean of > 50 cells per condition. Each individual point represents a single cell. Error bars represent the SEM. Statistics source data are in supplementary table S2. Scale bar = 5 mm.

Figure S6 Protein level expression of the fission yeast rescue constructs. Immuno-blot to quantify levels of each GFP-tagged rescue variant, visualized with a GFP antibody. b-actin is used as a loading control.

Figure S7 Uncropped image of blots from figure 1c, 3c, 4d, 5c, 6b.

Figure 1

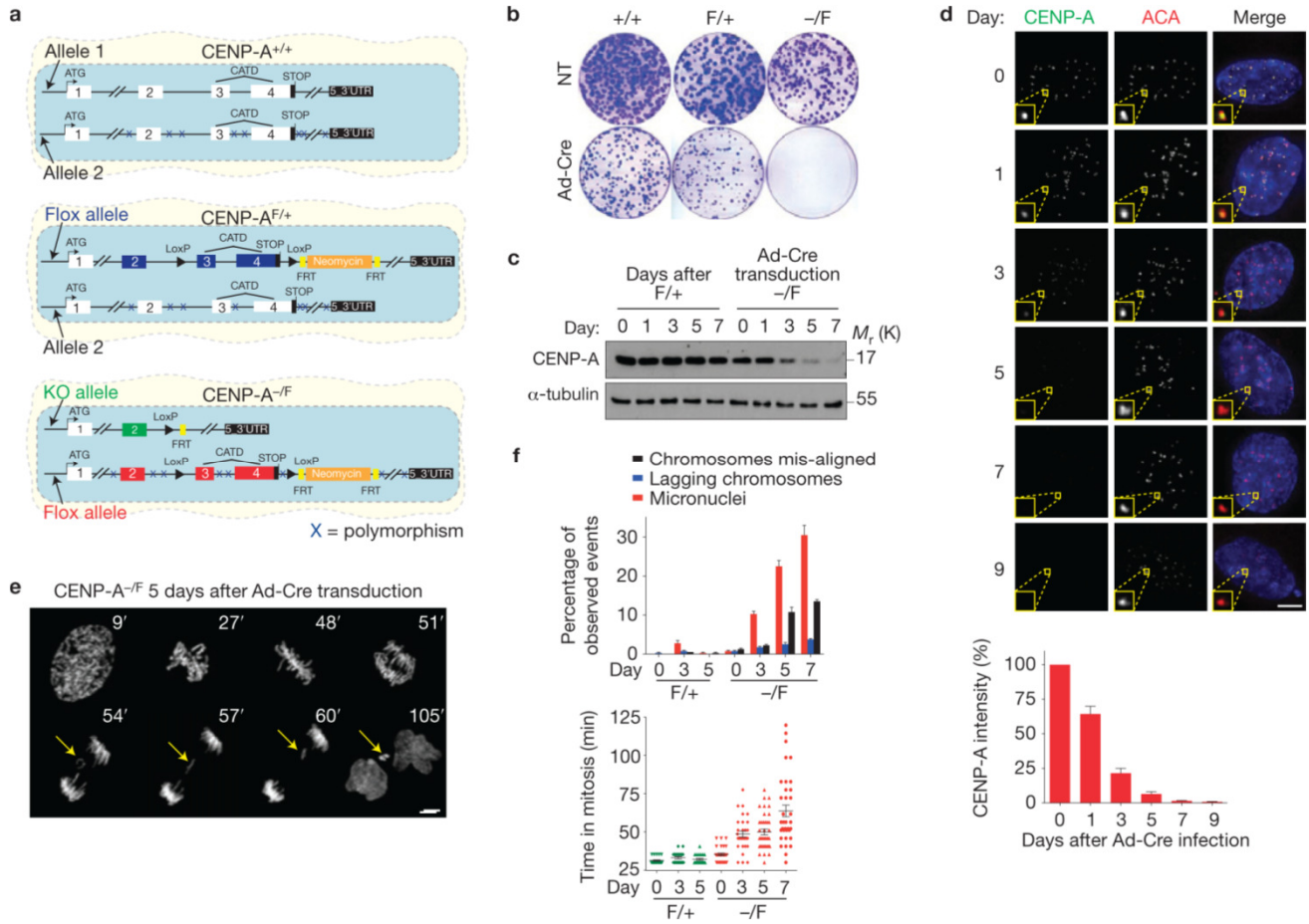


Figure 2

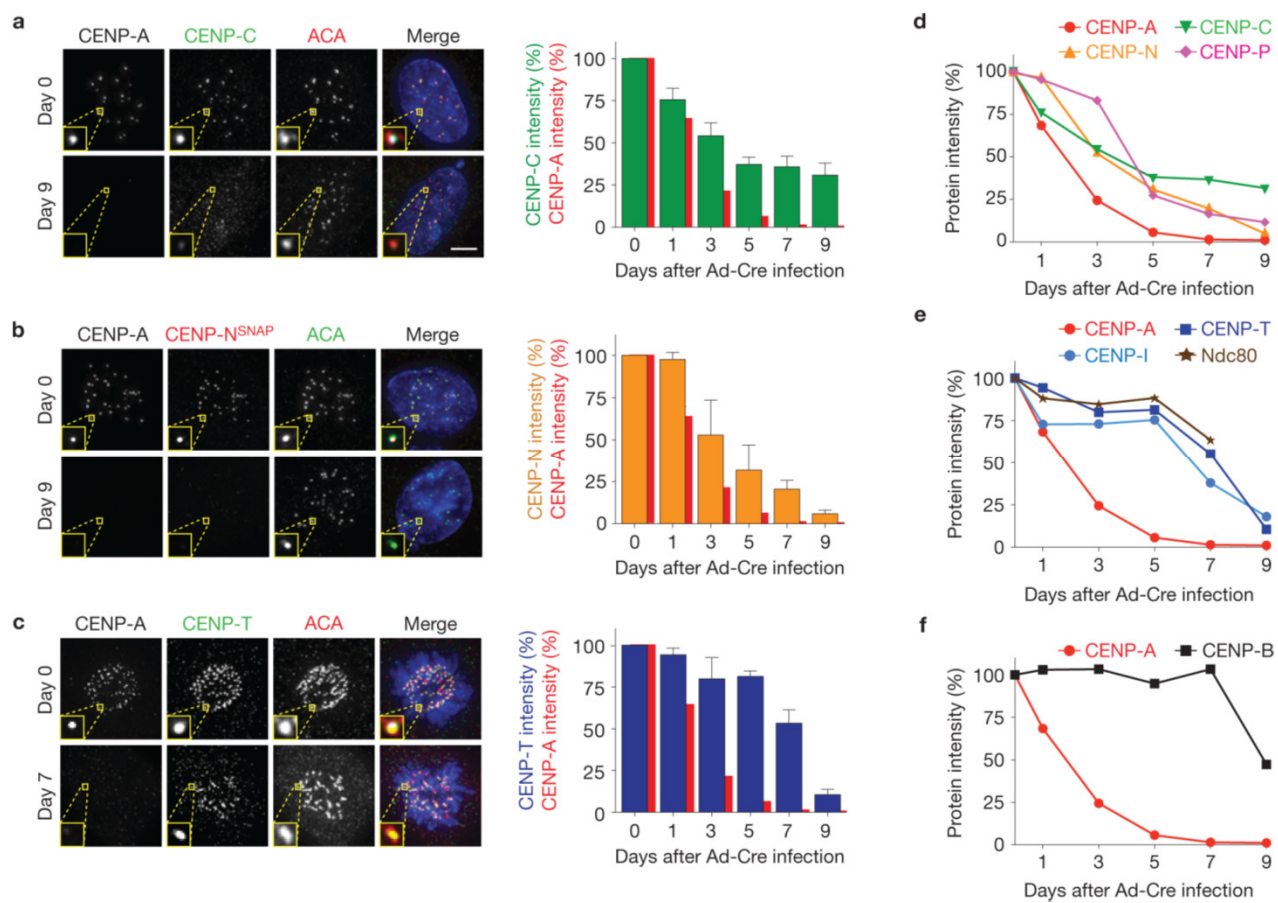


Figure 3

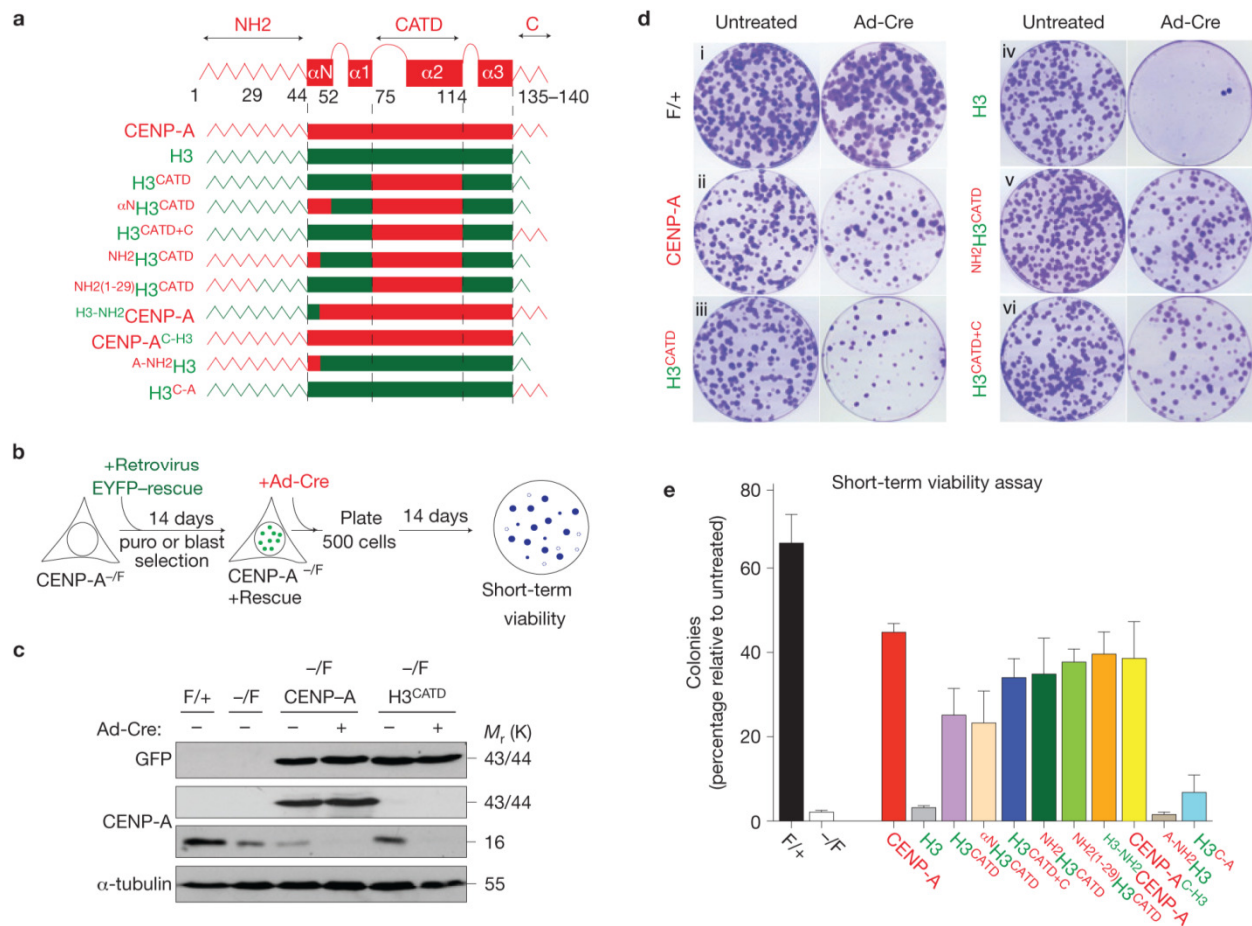


Figure 4

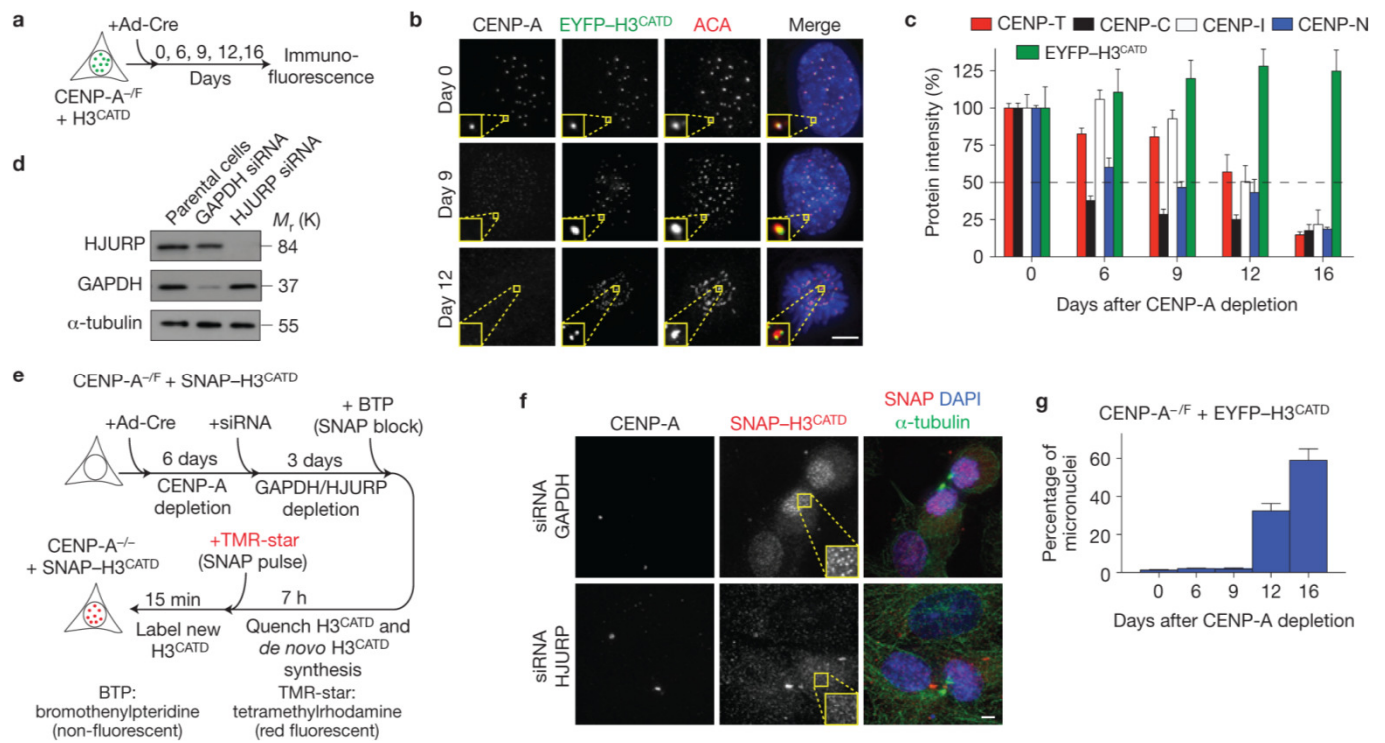


Figure 5

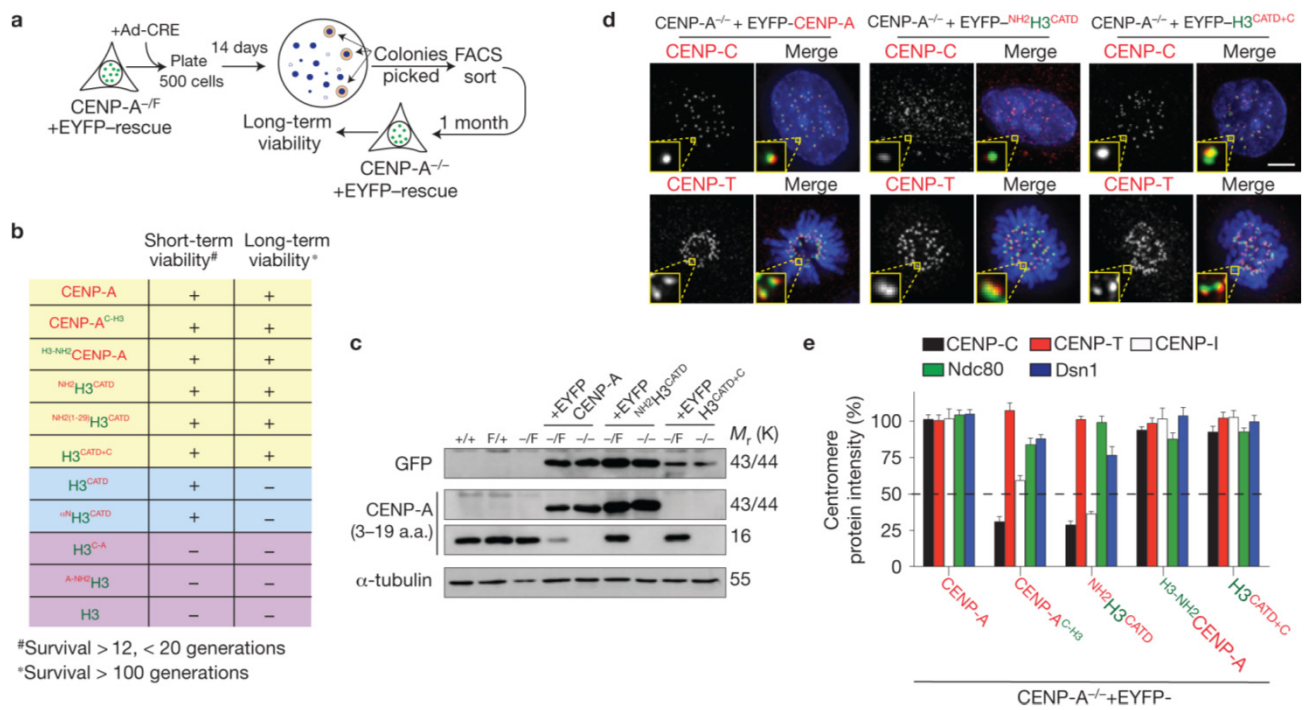


Figure 6

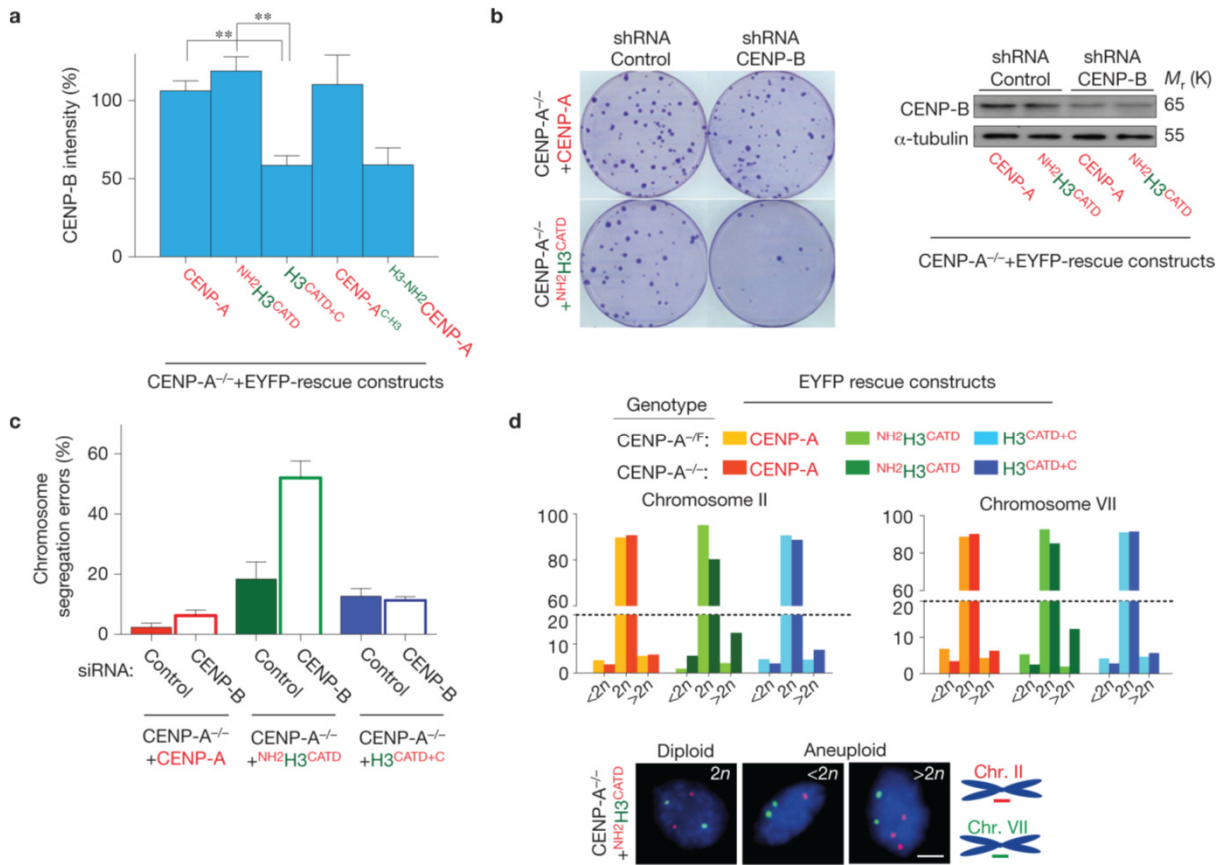


Figure 7

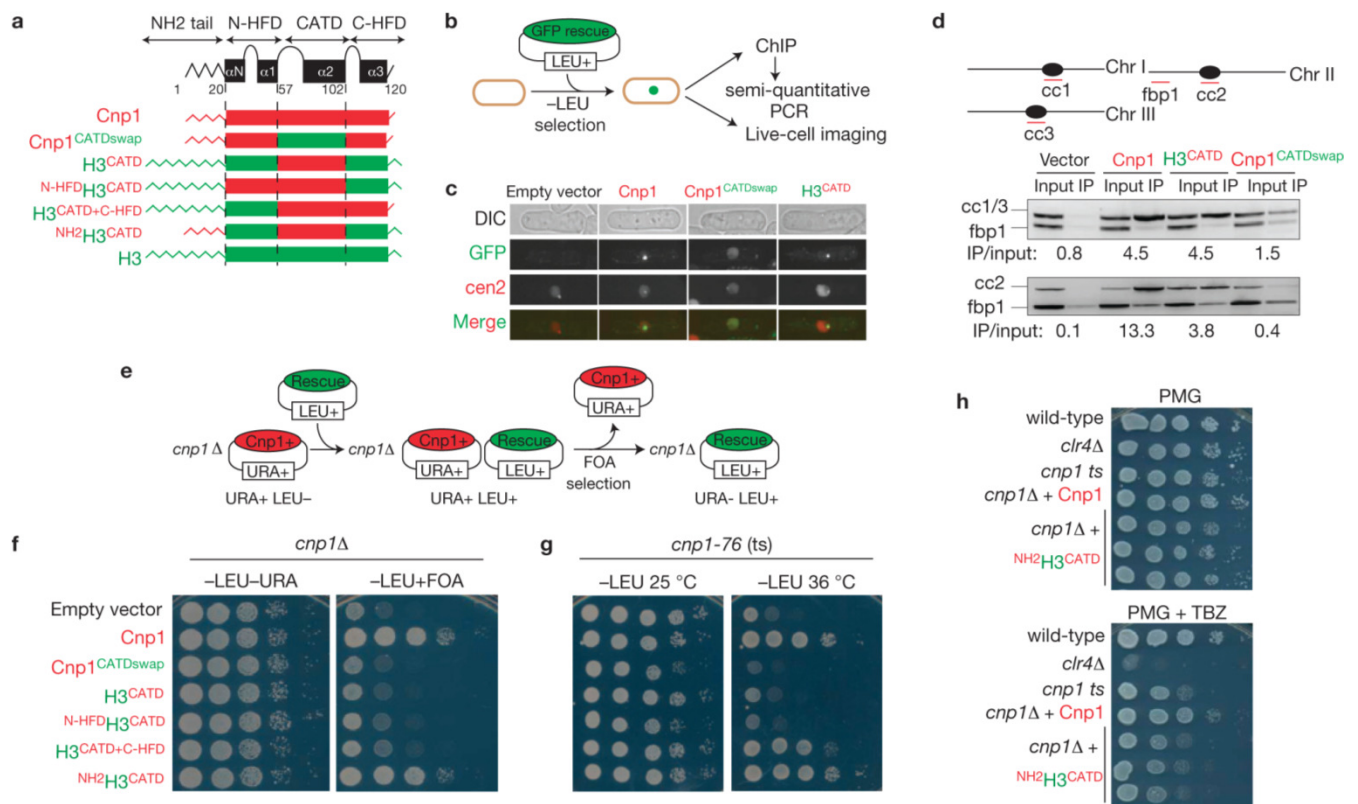


Figure 8

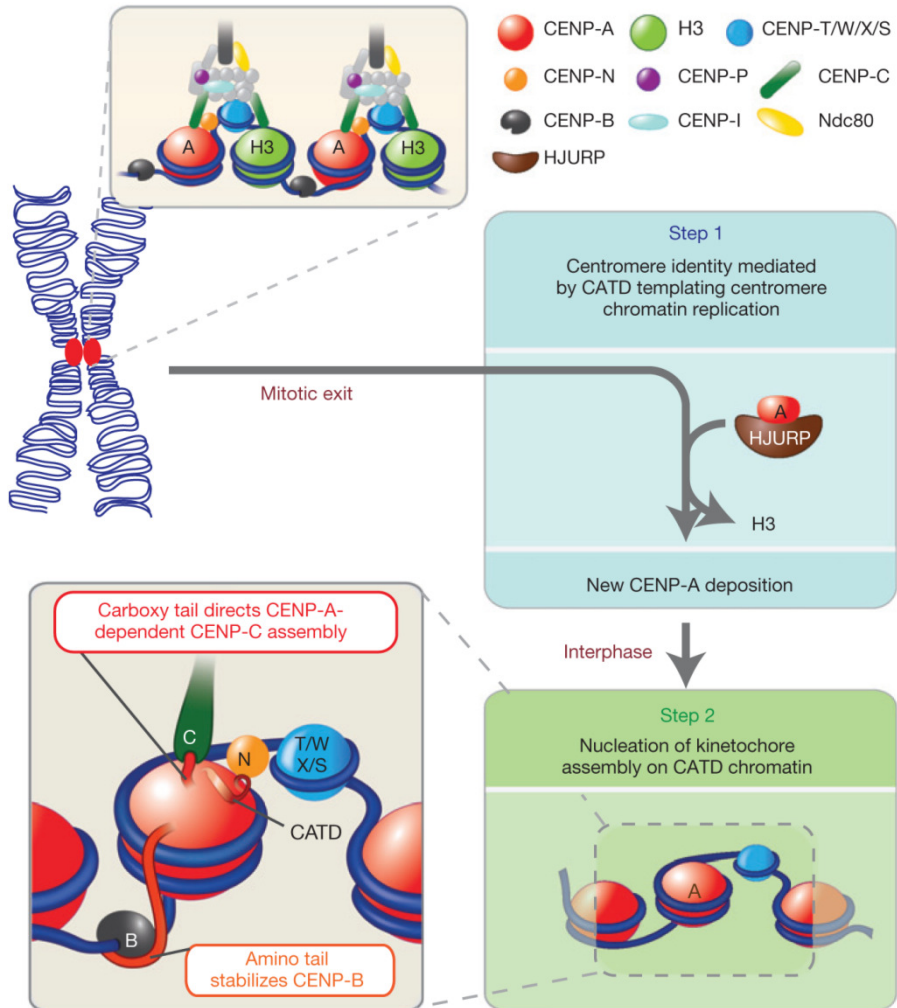
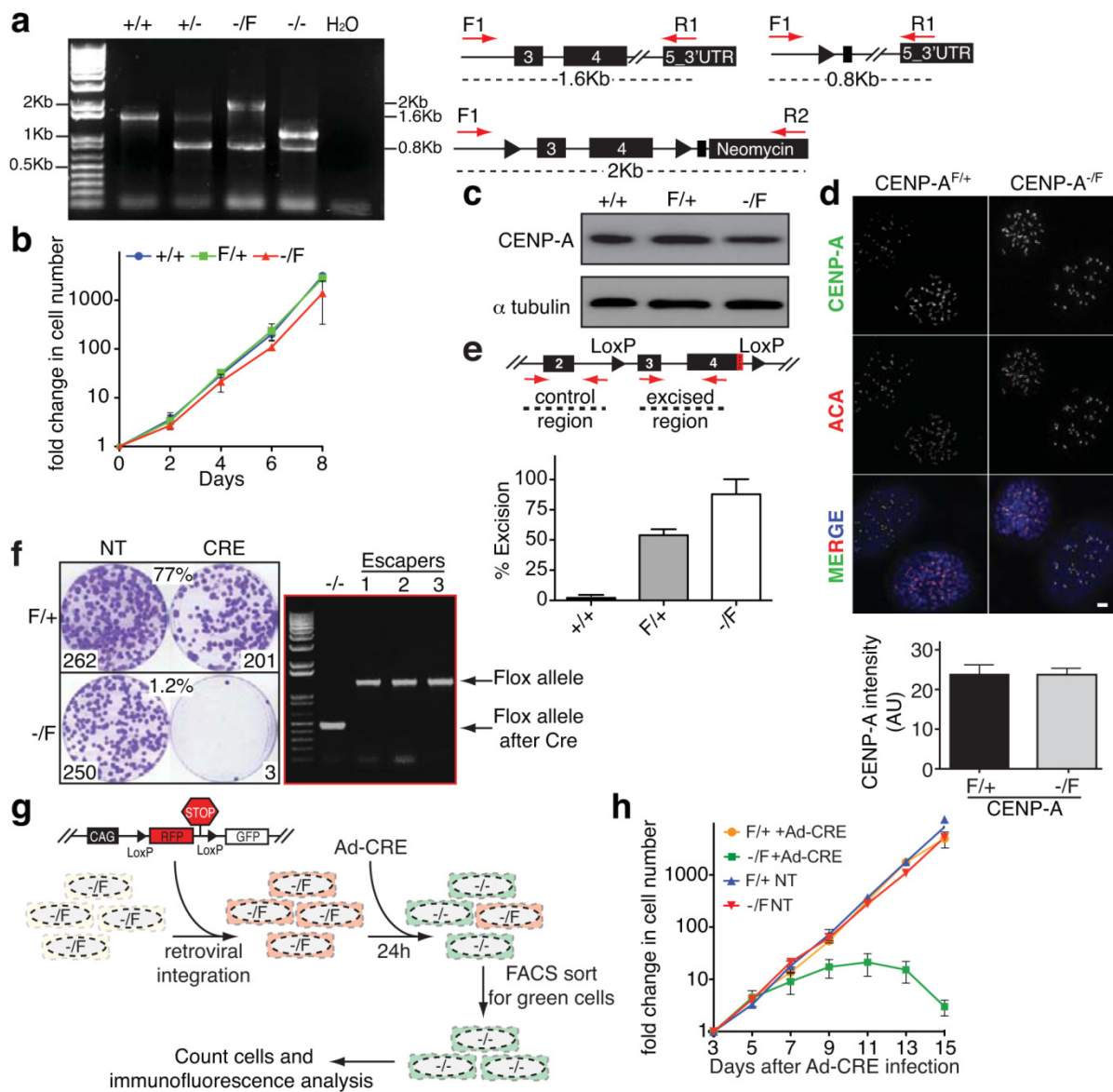


Figure S1



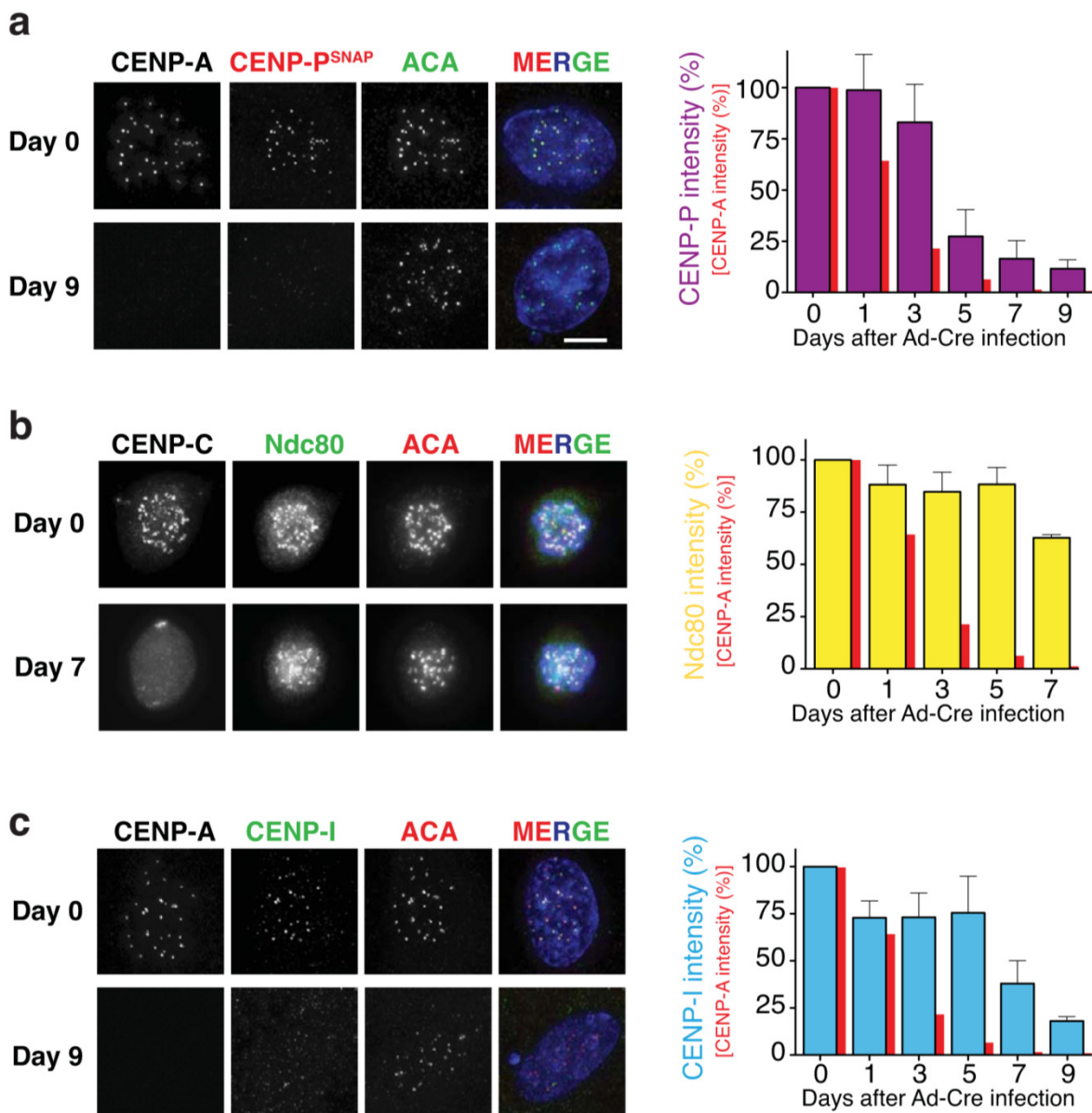
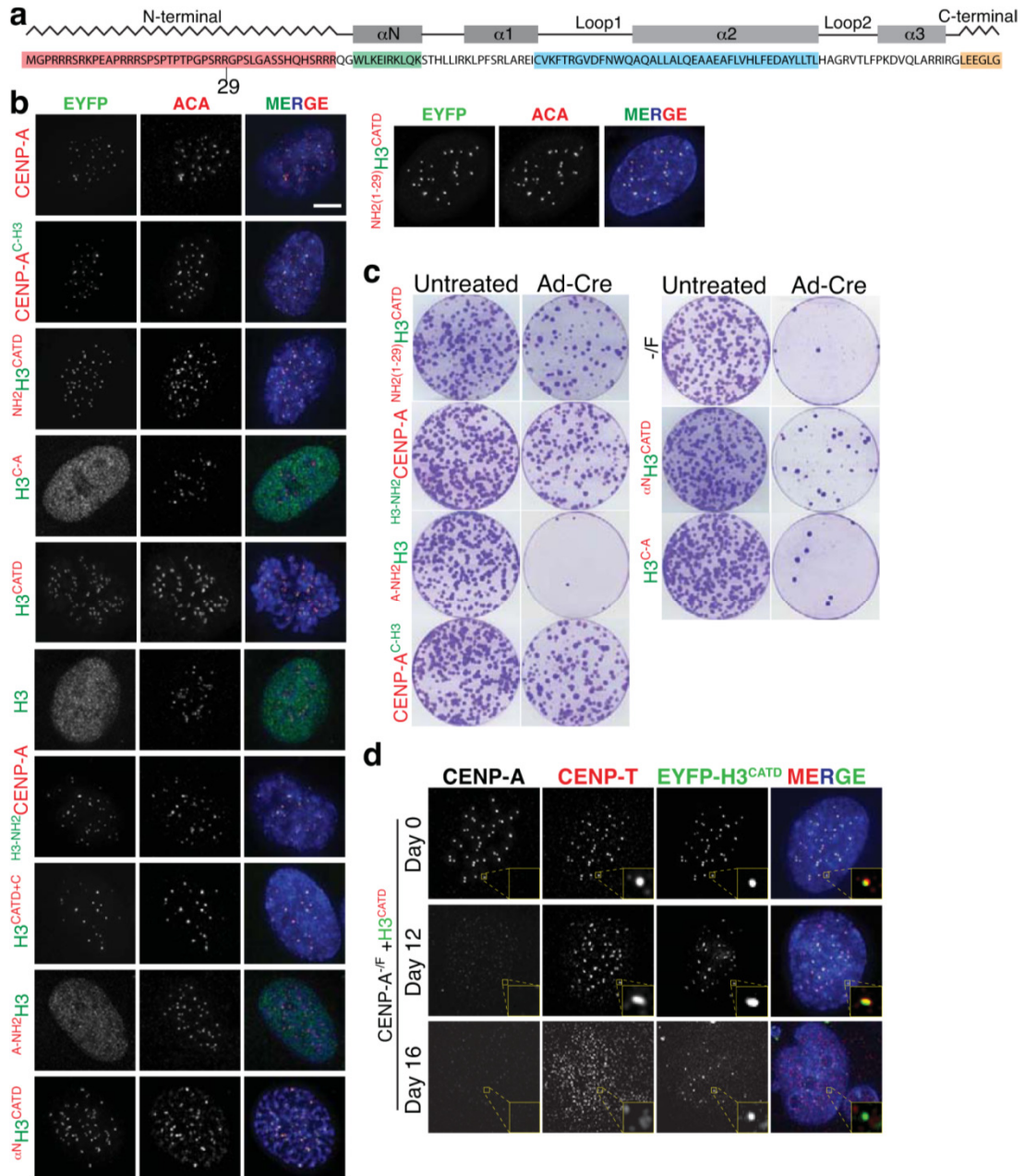
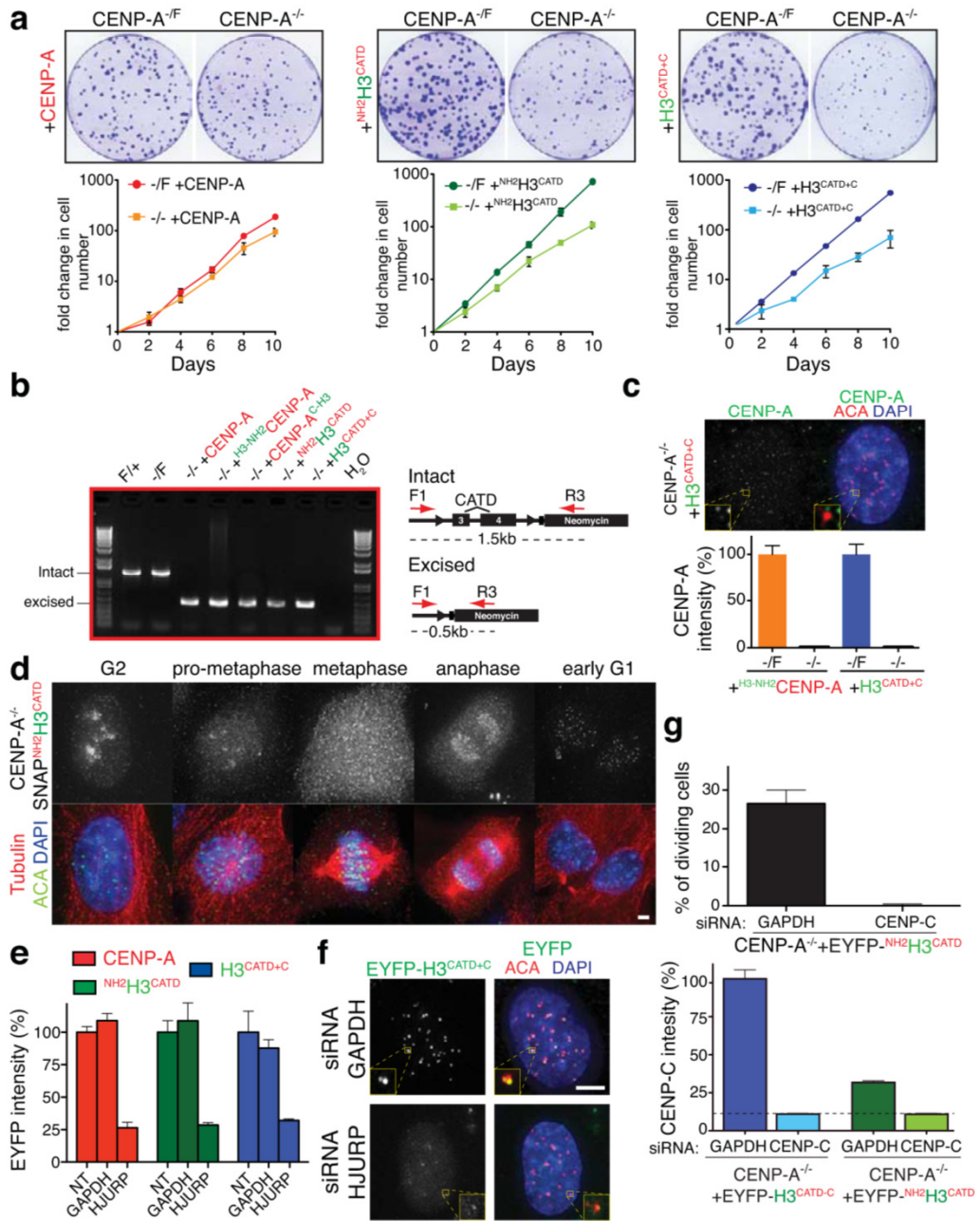


Figure S3





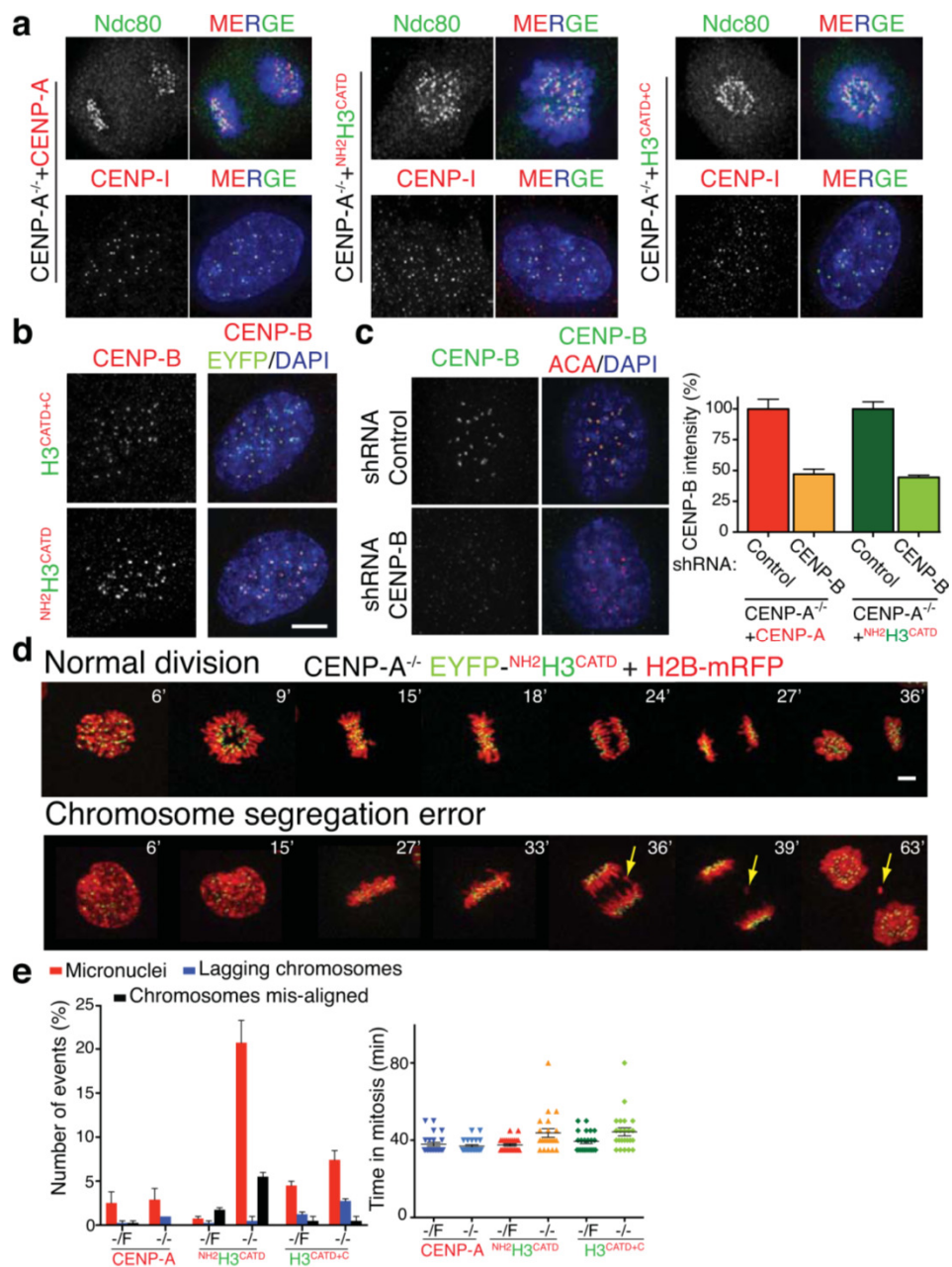


Figure S6

